The Dissertation Committee for Suvid Vikas Nadkarni Certifies that this is the approved version of the following dissertation:

ORGANIC TRANSISTOR BASED CIRCUITS AS DRIVERS FOR PLANAR MICROFLUIDIC DEVICES

Committee:

Ananth Dodabalapur, Supervisor

Jack C. Lee

Ray T. Chen

Dean P. Neikirk

Yueh-Lin (Lynn) Loo

Organic Transistor based Circuits as Drivers for Planar Microfluidic Devices

by

Suvid Vikas Nadkarni, B.E.; M.S.E.

Dissertation

Presented to the Faculty of the Graduate School of

The University of Texas at Austin

in Partial Fulfillment

of the Requirements

for the Degree of

Doctor of Philosophy

The University of Texas at Austin

December, 2007

Dedication

To my parents

Mrs. Manjiri Nadkarni and Dr. Vikas Nadkarni

Acknowledgements

The journey through graduate school has been one of the most enriching experiences in my life so far. I have had the privilege and the honor of interacting with so many fine individuals with diverse technical and cultural backgrounds, brilliant people, yet very down to earth and friendly. The work put together in this dissertation would not have been possible but for the help, guidance, motivation, support and faith bestowed by so many people. I would like to thank all the people who have contributed in some way or another in making this work possible. Without any one of them, the journey would not have been as memorable as it has been.

I would like to express my most sincere gratitude towards my advisor Dr. Ananth Dodabalapur, whose guidance and supervision has been invaluable. This work was successfully completed thanks to his patience, enthusiasm and passion for science. He has not only been a great leader and supervisor but also a great philosopher, friend and guide. It has always been a great honor to be associated with Professor Dodabalapur. I will remain forever indebted to him for everything that he has done for me.

I would like to thank Dr. Dean Neikirk, Dr. Yueh Lin Loo, Dr. Jack C. Lee and Dr. Ray Chen for serving on my committee and providing valuable inputs and guidance in putting together this dissertation.

A lot of credit goes to all my colleagues from our group, who always helped me in every way they could, at every step. I would like to acknowledge with immense gratitude valuable inputs and contributions from Tae-Ho Jung, Debarshi Basu, Lawrence Dunn, Yeon Taek Jeong, Byungwook Yoo, Liang Wang, Daniel Fine, Deepak Sharma, Jacopo Testa, Christopher Lombardo, Ashwin Madgavkar, Jae Won Shim, Davianne Duarte, Shannon Lewis, Brian Cobb, Sebastian Schöfer and Dharmendar Reddy. It has

been a great pleasure working and hanging out with all of these wonderful people. Financial support from the Texas ATP grant, the SPRING grant, AFOSR/STTR grant, the Keck foundation and support from the Center for Nano Materials is gratefully acknowledged.

A very special thank you goes out to Jean Toll, Amy Pinkston, Gerlinde Sehne and Joyce Kokes for the role they play behind the scenes. I would also like to thank the team at the Microelectronics Research Center for all the support and help they provided over the course of my graduate career. I will always appreciate help from James Hitzfelder, William Fordyce, Marylene Palard, Johnny Johnson, William Ostler, William James, Terry Mattord, Kenneth Ziegler, Brenda Francis and other personnel at the MER. I would like to thank Chris and Maria for making sure our workspaces were kept clean.

A huge thank you note goes out to all my friends and colleagues in graduate school, who shared the burdens and anxieties, joys and sorrows during my time in Austin. Life in Austin would not have been as much fun and memorable, but for the amazing support from Vinit Ogale, Tanmay Patel, Mihir Anandpara, Sundar Subramanian and Nachiket Kharalkar. I would also like to thank Antony Sebastine, Sachin Joshi, Sriram Sambamurthy, Rahul Nadagouda and Ramyanshu Datta for some fun times.

Last, but definitely not the least by any measure, I would like to acknowledge with deepest gratitude, support from my family. My ever supportive sister Nivedita with her endless love and understanding, my dear parents for their unconditional love, support, patience and encouragement, my brother-in-law Arjun for his advice and for always providing lighter moments, my cousin Mohan for his support and of course, my lady love, Trupta, for her love, support and understanding. Her presence has added a new dimension to my life. Thank you all so much for being there for me, putting up with me

and believing in me throughout. I am indebted to you all for life for being such lovely human beings that you all are and for helping me stand right back on my feet, every time I fell.

Thank you all very much!

Organic Transistor based Circuits as Drivers for Planar Microfluidic Devices

Publication No._____

Suvid Vikas Nadkarni, Ph.D.

The University of Texas at Austin, 2007

Supervisor: Ananth Dodabalapur

The work presented in this dissertation is focused on integrating organic transistor based circuits with planar microfluidic devices for discrete droplet handling. Discrete droplet based microfluidic systems are being increasingly investigated for lab-on-a-chip type applications. An essential component of a lab-on-a-chip system is the drive circuitry that runs the system. Conventionally, a variety of schemes have been implemented for acting as drivers for microfluidic devices. Organic transistor based circuits offer a viable and cost-effective option for serving as drivers for planar microfluidic devices. The magnitudes of voltages and the time scales involved in implementing these discrete droplet based systems are in good agreement with the values of voltages that can be reliably generated using organic transistor based circuits. Thus, the union of two cost-effective technologies with the ability to perform a wide variety of functions in a lab-on-a-chip type system would be highly desirable.

A simple, planar microfluidic device with an open structure is implemented on a glass substrate. The device is optimized for reliable and repeatable performance using Cytop as the insulating dielectric. Cytop provides a highly hydrophobic surface for reversible wetting to take place on the application of electrical voltage. Various organic transistor based circuits are fabricated using Pentacene as the p-type semiconducting material and N,N' –bis(n-octyl)-dicyanoperylene-3,4:9,10-bis(dicarboximide) (PDI-8CN_2) as the n-type material. A top contact inverter, which is the most basic complementary metal oxide semiconductor circuit is fabricated and used as the driver for the planar microfluidic device. The output voltages generated by the inverter are used to actuate discrete water droplets over adjacent electrodes and also to perform merging of droplets, which is another basic functional operation that is performed on lab-on-a-chip type assemblies. Reliable and repeatable performance of the microfluidic device as well as the CMOS circuit is achieved. This work presents the first implementation of a discrete droplet based device driven by electrical voltages generated by an organic transistor based circuit. The physical mechanisms that are responsible for the motion of droplets have been investigated and contributions from electrowetting forces and dielectrophoretic forces have been resolved.

Table of Contents

List of Figures

CHAPTER 1: INTRODUCTION

1.1 Background

Experimentation with plastics has been carried out by mankind since a very long time. Plastics are essentially polymers, long chains of atoms bonded together with carbon and hydrogen atoms forming the backbone in a vast majority of polymeric materials [1]. Plastics have worked their way into being an indispensable part of our daily lives finding applications in textiles, food packaging, automobiles, electronics, etc. Plastics are primarily used as insulators in most electronics-related applications. However, the Nobel prize-winning discovery of conducting polymers in 1977 by Alan J. Heeger, Alan MacDiarmid and Hideki Shirakawa opened up a whole new area for research on plastics with potentially numerous applications [2, 3]. This landmark discovery also gave impetus to the study of the electrical properties of conjugated organic molecules.

Research on organic semiconducting materials and conjugated polymers, from their synthesis to applications is being extensively carried out by a number of groups in the world. Electronic devices fabricated from organic and polymer semiconducting devices have myriad applications in organic light emitting diodes (OLED's), photovoltaics, radio-frequency identification tags (RFID), chemical and biological sensing and large-scale complementary circuits [4-8]. The implementation of organic devices and circuits offer significant advantages over their conventional inorganic counterparts in terms of ease of fabrication, low cost and potential for large-scale roll-to-

roll processing. Another significant feature offered by organic and polymer semiconducting devices is the ability to fabricate such devices and circuits on a variety of substrates. Fabrication of low cost, large-area applications is made efficient and less complex using additive methods such as printing [9, 10]. Printing may add some complexity to the fabrication process but is a cost-effective technique.

1.2 Organic Semiconducting Materials

Depending upon the arrangement of molecules and the nature of majority charge carriers, organic semiconductors can be either p-type or n-type. Polycrystalline organic thin-films transport one type of carrier. Some materials are also known to exhibit anisotropy in their transport properties, favoring hole transport in one direction and electron transport in another [11]. However, due to the trapping of one type of carrier, certain organic materials exhibit predominantly n-type behavior and certain others exhibit p-type behavior. The majority carriers in p-type semiconductors are holes whereas the majority carriers in n-type semiconductors are electrons [12]. Organic materials get their semiconducting properties from conjugated π-bonds present in the constituent molecules. There is usually a high degree of order in organic crystals, particularly thin crystalline films. Crystal order along with π-orbital overlap makes it easy for charges to move between molecules. This results in a good mechanism for conduction in organic materials. The constituent molecules in organic semiconductors are bonded by weak Van der Waals forces in contrast to inorganic materials which are formed by covalent or ionic

bonding between elements. Organic semiconductors can be synthesized in a desired fashion at the molecular level and suitable selections of structural units can be made to achieve the required properties. Some of the commonly used organic and polymer semiconducting materials that show reliable and good performance characteristics for devices are shown in Fig. 1.1. [13]

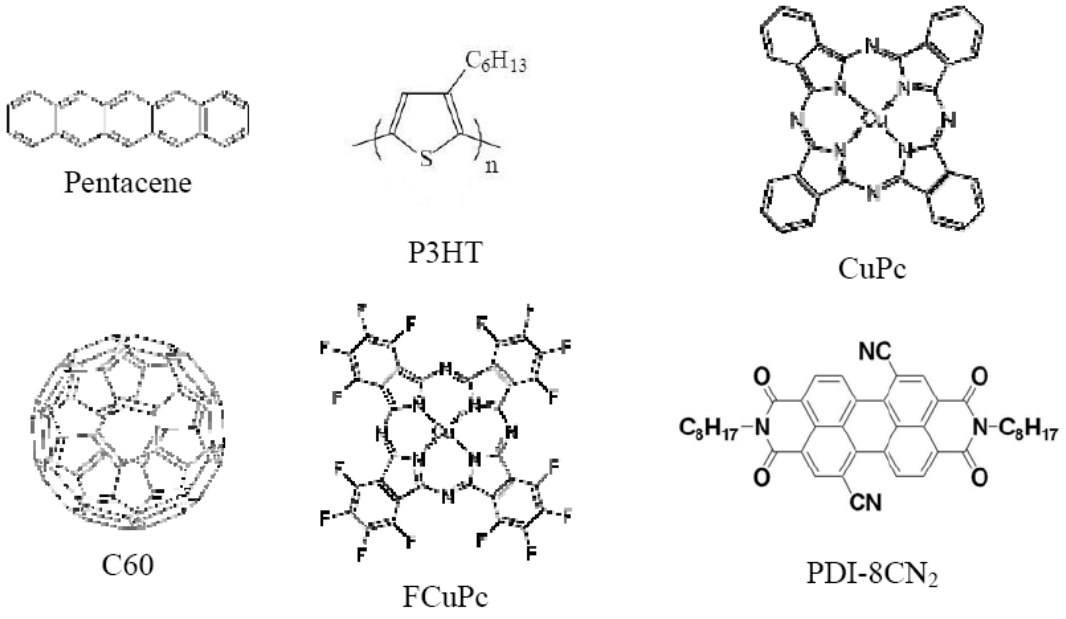

Figure 1.1: Commonly used high-performance organic and polymer semiconducting materials.

P-type semiconductors such as pentacene, regioregular poly(3-hexylthiophene) (P3HT), and rubrene have been extensively researched and are the commonly used p-type materials in most organic devices. It is necessary to have good, high performance n-type materials specifically for applications such as organic light emitting diodes and organic complementary metal oxide semiconductor (CMOS) circuits. Some of the n-type

materials used for these applications include N,N'-bis(n-octyl)-dicyanoperylene-3,4:9,10-bis(dicarboximide) (PDI-8CN_2), copper hexadecafluorophthalocyanine (F_{16}CuPc), and C_{60}. Carbonyl functionalized (α,ω-diperfluorohexyl-4T) (DFHCO-4T) is another n-type material that has been used in fabricating inverters.

1.3 Transport in Organic Semiconductors

The primary difference between organic semiconducting materials and inorganic semiconductors is the nature of charge transport that is responsible for conduction. The nature of charge transport in inorganic semiconductors such as silicon is band-like as the system has definite order. The charge carrier mobilities are very high, of the order of 10^3 cm^2/Vs at room temperature. The charge carrier mobilities in organic semiconductors are orders of magnitude lower than the mobilities in inorganic materials. Mobility in inorganic materials reduces with increasing temperature because the lattice vibrations (phonons) cause scattering. The nature of transport in organics is more of the hopping kind. Crystalline organic semiconductors can have band-like transport at low temperatures. The molecules are bound together by weaker Van der Waals forces resulting in a weaker interaction. At high temperatures, due to strong electron-phonon interaction, the bandwidths shrink and band transport ceases even in high quality crystals. In disordered materials, a variety of trap states lower the mobility further. Energy states are localized in disordered organic materials and charge transfer takes place by hopping. Due to the charge carrier scattering at every step, the carrier mobilities are significantly

lower. In this case, the mobility is inversely dependent on temperature as hopping transport is assisted by phonons [14, 15].

There is an intermediate stage in partially ordered organic semiconductors. Due to the poly-crystalline nature of organic thin-films, there is order present in small sections of the film called grains which are separated by grain boundaries that act as trapping centers of charge carriers. Figure 1.2 shows an AFM image of a Pentacene film clearly indicating the presence of grains and grain boundaries.

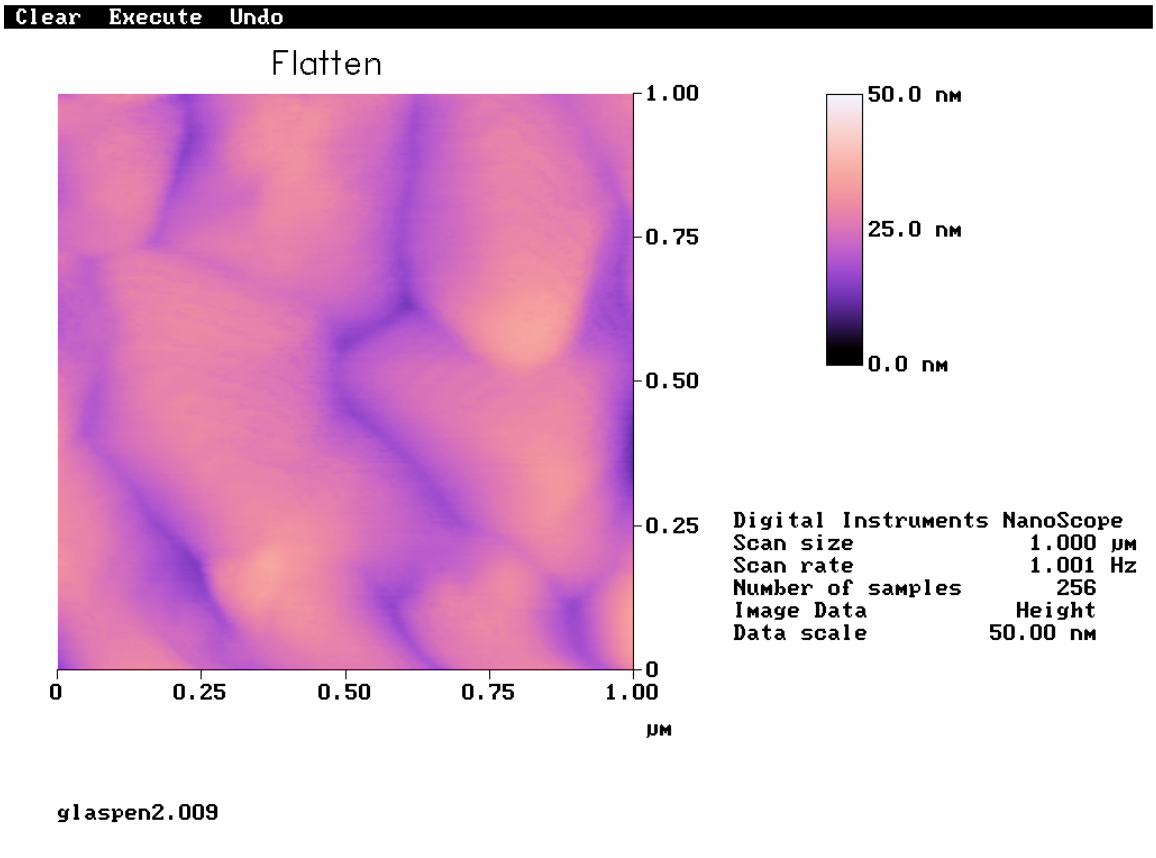

Figure 1.2: AFM image showing a 1µm scan of a Pentacene film. The grain size is ~ 0.5 µm.

The transport model employed for explaining charge carrier transport in organic semiconductors is the Multiple Trapping and Release (MTR) model [16]. The model suggests distributions of traps in the forbidden energy gap above the valence band edge. At low gate voltages, a majority of charge carriers injected in the semiconductor get trapped in these localized states with the deep traps filling up first. As the gate voltage is increased, more traps get successively filled and the Fermi level approaches the valence band edge. In some cases, when a sufficiently high gate voltage is achieved, all trap states are filled and the subsequently injected carriers move with the mobility associated with carriers in the valence band [17, 18]. However, the temperature-independent mobility reported in some cases (Pentacene and oligothiophenes) is not accounted for by the MTR model [19-21]. Thus, the mechanisms for charge transport between molecules could be band-like transport, hopping, or tunneling [22-25]. At room temperature, the condition for band transport is $\mu \geq 1$ cm^2/Vs. If $\mu < 1$ cm^2/Vs, the nature/type of transport is hopping [20, 26].

The charge carrier mobilities in organic semiconductors do not place these materials in the same league as silicon from the point of view of applications. Organic semiconducting devices have niche application areas of their own and provide a viable alternative to conventional technologies in several areas that are discussed in the next section.

1.4 Application Areas

Organic materials are used as semiconducting materials as well as insulators. These form the basic working components in an organic field effect transistor (OFET). Organic transistors form the basic element of several applications involving organic materials. OFET's are of great interest because of their potential use in low-cost, large-area circuits on flexible substrates. With new materials being synthesized for higher charge carrier mobilities, the range of applications for OFET's becomes broader. As mentioned earlier, such applications include chemical sensors [27], photodetectors [28] and display devices [29]. An active matrix display integrating OFET's with OLED's into smart pixels is an attractive application from the consumer electronics point of view [30]. Organic transistors also find use in non-LED based display applications such as electronic paper [31]. A prototype electronic paper display has been made by the E-Ink Corporation [32]. Organic transistor based active matrix has also been used in making a large-area array of thermal and pressure sensors [33]. This sensor array has been implemented in making 'artificial' skin by Someya *et al* in making a bionic hand [34].

Electronic circuits fabricated from organic transistors are also an important application. With the synthesis of high performance n-type semiconducting materials, complementary metal oxide semiconductor (CMOS) circuits are performing better and with higher reliability. CMOS circuits are preferred over PMOS circuits due to the fact that they have low power consumption and higher nose margins. Until recently, most

research had been focused towards p-type semiconducting materials and PMOS circuits due to the fact that there were not many air-stable n-type materials that were available, that showed good performance characteristics. Large-scale CMOS integrated circuits have been implemented using a variety of n-type and p-type semiconducting materials [35].

The switching speeds achieved in organic transistor based circuits are not comparable to the switching speeds achieved in circuits using conventional silicon technology. However, as mentioned before, there is a unique set of application areas in which organic transistor based circuits are the prefect candidate. One such application area is the potential shown by these circuits to act as drivers for microfluidic devices based. The voltage levels that can be generated using organic circuits are in perfect agreement with the voltages required for running discrete droplet based microfluidic devices, which in itself, has several application areas in lab-on-a-chip technologies.

1.5 Dissertation Organization

Having touched on the basics of organic semiconducting materials, the nature of charge transport in these materials and the various application areas of organic materials, the following chapters are devoted to discussing organic devices and circuits and a new application of organic transistor based circuits in acting as drivers for planar microfluidic devices. Chapter 2 discusses basics of organic transistors and circuits. The basic structure and device geometries of organic transistors are discussed along with the nature of the electrical characteristics. Organic transistors form the basic building blocks of organic circuits, which have a wide range of applications. The focus of this research is the integration of organic transistor based circuits with discrete droplet based microfluidic devices. With that knowledge, Chapter 3 is devoted to an overview on microfluidic systems. Conventional schemes for the implementation of such systems are discussed along with their advantages and drawbacks. Chapter 4 is devoted to the planar microfluidic device implemented for discrete droplet handling. Various design considerations in the implementation of such a device are addressed. The fabrication procedure and testing methodology is discussed followed by the integration of this device with an organic transistor based circuit in Chapter 5. Chapter 5 also discusses the fabrication and characterization of other organic transistor based circuits which can be implemented in the future for driving microfluidic systems. The eventual aim of pursuing research in this area is development of a lab-on-a-chip system that will be a self-sufficient and completely functional system performing various operations on a single chip, with all

the processing systems and driver systems integrated on to one single chip. The first steps towards realization of this objective have been taken. A lot of parameters go into the design and implementation of such systems. The work reported in this research addresses a new application area for organic transistor based circuits, bearing in mind the ever-present goals of coming up with a cost-effective and reliable technology. A summary of the research work carried out is given in Chapter 6 with a brief discussion on future directions for work in this area.

1.6 References

[1] http://en.wikipedia.org/wiki/Plastic referenced from Wikipedia

[2] A.G. MacDiarmid, M. Akhtar, C.K. Chiang, M.J. Cohen, J. Kleppinger, A.J. Heeger, E.J. Louis, J. Milliken, M.J. Moran, D.L. Peebles, and H. Shirakawa, J. Electrochem. Soc., 124, C304 (1977)

[3] H. Shirakawa, E.J. Louis, A. G. MacDiarmid, C. K. Chiang, A. J. Heeger, J. Chem. Soc. Chem. Commun., 16, 578 (1977)

[4] Robert Rotzoll, Siddharth Mohapatra, Viorel Olariu, Robert Wenz, Michelle Grigas, Klaus Dimmler, Oleg Shchekin and Ananth Dodabalapur, Applied Physics Letters 88, 123502 (2006)

[5] Liang Wang, Daniel Fine, Deepak Sharma, Luisa Torsi and Ananth Dodabalapur, Analytical and Bioanalytical Chemistry 384, 310 (2006)

[6] B. Crone, A. Dodabalapur, Y.Y. Lin, R. W. Filas, Z. Bao, A. LaDuca, R. Sarpeshkar, H. E. Katz and W. Li, Nature 403, 521 (2000)

[7] C. J. Brabec, Solar energy materials and solar cells, 83, 273 (2004)

[8] J. H. Burroughes, D. D. C. Bradley, A. R. Brown, R. N. Marks, K. Mackay, R. H. Friend, P. L. Burns and A. B. Holmes, Nature 347, 539 (1990)

[9] Rogers, J.A.; Bao, Z.; Baldwin, K.; Dodabalapur, A.; Crone, B.; Raju, V.R.; Katz, H.E.; Kuck, V.J.; Amundson, K.; Ewing, J.; Drzaic, P. Proc. Nat. Acad. Sci. **98**, 4835-4840 (2001)

[10] J. A. Rogers and Z. Bao, Journal of Polymer Science Part A: Polymer Chemistry 40 (20), 3327 (2002)

[11] J. R. Ostrick, A. Dodabalapur, L. Torsi, A. J. Lovinger, E. W. Kwock, T. M. Miller, M. Galvin, M. Berggren and H. E. Katz, Journal of Applied Physics, 81, 10, 6804 (1997)

[12] C. D. Dimitrakopoulos and P. R. L. Malenfant, Advanced Materials, Vol. 14, No. 2, pp. 99-117 (2002)

[13] Tae Ho Jung, Submicron and nanoscale organic field-effect transistors and circuits, PhD Dissertation (2006)

[14] S. Jeyadev and E.M. Conwell, Phys. Rev. B, 35, 6253 (1987)

[15] E.M. Conwell, H.Y. Choi, and S. Jeyadev, Synth. Metals, 49, 359 (1992)

[16] P.G. Le Comber and W. E. Spear, Phys. Rev. Lett., 25, 509 (1970)

[17] C.D. Dimitrakopoulos, J. Kymissis, S. Purushothaman, D.A. Neumayer, P.R. Duncombe, and R.B. Laibowitz, Adv. Mater., 11, 1372 (1999)

[18] C.D. Dimitrakopoulos, S. Purushothaman, J. Kymissis, A. Callegari, and J.M. Shaw, Science, 283, 822 (1999)

[19] G. Horowitz, M.E. Hajlaoui, and R. Hajlaoui, J. Appl. Phys. 87, 4456 (2000)

[20] S.F. Nelson, Y.Y. Lin, D.J. Gundlach, and T.N. Jackson, Appl. Phys. Lett., 72, 1854 (1998)

[21] G. Horowitz, R. Hajlaoui, R. Bourguiga, and M.E. Hajlaoui, Synth. Metal, 101, 401 (1999)

[22] N. Karl, J. Marktanner, R. Stehle, and W. Warta, Synth. Metal, 42, 2473 (1991)

[23] D. Emin, Phys. Rev. Lett., 25, 1751 (1970)

[24] T. Holstein, Ann. Phys. (N.Y.), 8, 325 (1959)

[25] R. M. Glaser and R. S. Berry, J. Chem. Phys., 44, 3797 (1966)

[26] G. Horowitz, Adv. Mater., 10, 3 (1998)

[27] B. Crone, A. Dodabalapur, A. Gelperin, L. Torsi, H. E. Katz, A. J. Lovinger and Z. Bao, Applied Physics Letters, 78, 2229 (2001)

[28] P. Peumans, V. Bulovic and S. R. Forrest, Applied Physics Letters, 76, 3855 (2000)

[29] C. W. Tang and S. A. VanSlyke, Applied Physics Letters, 51, 913 (1987)

[30] K. Tsukagoshi, J. Tanabe, I. Yagi, K. Shigeto, K. Yanagisawa and Y. Aoyagi, Journal of Applied Physics, 99, 064506 (2006)

[31] Y. Chen, J. Au, P. Kazlas, A. Ritenour, H. Gates and M. McCreary, Nature, 423, 136 (2003)

[32] http://en.wikipedia.org/wiki/Electronic_paper referenced from Wikipedia

[33] Takao Someya, Yusaku Kato, Tsuyoshi Sekitani, Shingo Iba, Yoshiaki Noguchi, Yousuke Murase, Hiroshi Kawaguchi and Takayasu Sakurai, Proceedings of the National Academy of Sciences vol. 102, no. 35, 12321 (2005)

[34]http://www.ntech.t.utokyo.ac.jp/Archive/Archive_download/pictures/artificial_skin3.jpg referenced from Wikipedia

[35] B. Crone , A. Dodabalapur, Y. Y. Lin, R. W. Filas, Z. Bao, A. LaDuca, R. Sarpeshkar, H. E. Katz and W. Li, Nature vol. 403, no. 6769,521 (2000)

CHAPTER 2: ORGANIC TRANSISTORS AND CIRCUITS

2.1 Introduction

Organic semiconductors have many properties which make them viable alternatives in a number of applications. Some of the advantages of using organic semiconductors are their compatibility with a large number of substrates from silicon to plastics, easy processing and the leeway offered by the materials in making structural modifications [1]. Organic materials get their semiconducting properties due to conjugated π-bonds. There is also a high degree of order in organic crystals. Crystal order along with π-orbital overlap makes it easy for charges to move between molecules. Thus, there is a good mechanism for conduction in organic materials.

Organic thin film transistors are made by using these materials as the active layers. Depending upon the type of semiconductor used, the TFT is either p-type or n-type. Whichever the type of the semiconductor, there are many properties that it must possess so as to function as desired. The semiconducting material must accept charge from the source electrode without a high barrier and the charge should move rapidly through the channel with an acceptable mobility. The charge density should be conveniently modulated using reasonable gate voltage levels [2]. A very important attribute that the semiconducting material must possess is the ability to withstand operating conditions without thermal, electro-chemical or photo-chemical degradation [2]. A reasonable voltage level is one that can give sufficient driving force to the charge

carrier to propagate through the channel. Analogous to the Valence Band and Conduction Band in inorganic semiconductors, organic semiconductors possess highest occupied molecular orbital (HOMO) and lowest unoccupied molecular orbital (LUMO) respectively. Hence, the HOMO and LUMO levels should be so aligned that the transfer of holes or electrons takes place without creating a chemical imbalance [2].

2.2 Organic Thin-Film Transistors

Organic thin-film transistors were first demonstrated in 1983 by Ebisawa et al [3]. Since the first implementation of an OTFT, a lot of research has been carried out in the fabrication and characterization of OFETs, using different materials. These thin-film transistors have attracted considerable attention for use in a wide range of cost effective, high volume applications such as radio-frequency identification tags, display drivers, smart cards, organic light-emitting diodes, solar cells, sensor arrays, electronic paper and photodetectors [4-11]. The areas of focus in thin-film transistors include studies on the semiconducting materials, synthesis of new materials such as thiophene derivatives, use of organic insulating layers, polymer source-drain contacts, fabrication and characterization of sub-micron and nanoscale transistors and the fabrication of submicron OFETs by nanoimprint lithography [7, 12-17]. The spectrum of applications using organic thin film transistors broadens as new materials are synthesized and cost effective techniques of fabrication using additive methods such as solution processing and printing are being developed. For making OFETs in commercially viable applications such as

display drivers, the electrical properties of the semiconducting materials have to be improved. In terms of device performance, the materials have to be air stable and give a repeatable and reliable performance in terms of transistor operation. The most important parameters for the implementation of good working devices are the charge carrier mobility and the current on/off ratio of the organic thin film transistors.

2.3 Device Geometries of Organic Transistors

The geometry of the organic thin-film transistor (OTFT) differs from the conventional silicon-based metal-oxide-semiconductor field-effect transistor (MOSFET). Typically two standard device geometries are employed while fabricating organic thin film transistors. The device can either be made as a top contact device as shown in Figure 2.1(a) or a bottom contact device as shown in Figure 2.1(b).

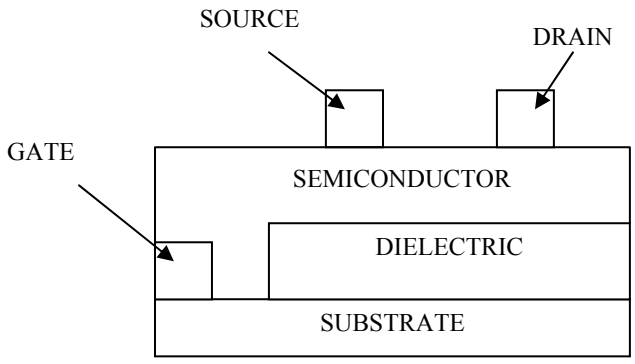

Figure 2.1(a): Top-contact configuration.

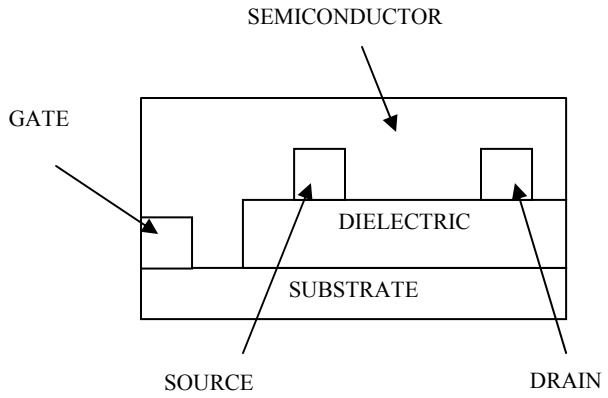

Figure 2.1(b): Bottom-contact configuration.

The two configurations are so named as a result of the portion of the semiconductor that is in contact with the metal electrodes. In the top-contact configuration, the source and drain electrodes are patterned above the semiconductor where as in the bottom-contact configuration, the semiconductor is deposited over the source and drain electrodes as shown in the Figure 2.1(b). Thus, the area of the electrodes in contact with the semiconductor is more in the bottom-contact configuration. Consequently, charge injection from the electrodes takes place in the lateral as well as the perpendicular direction. In the top-contact configuration, there is only a lateral movement of the charge. The top-contact configuration usually has a critical advantage of better metal-semiconductor charge transfer over the bottom-contact configuration [2].

The dielectric generally used is silicon dioxide. The metal electrodes used are generally Gold, Silver or Aluminum. As listed in the previous section, there is a wide variety of organic semiconductors that can be used as the active layer in these devices. Of the many p-type organic semiconductors that have been researched over the years, Pentacene is one organic material that has been extensively studied.

The performance of the top-contact and the bottom-contact configurations is generally different in OTFTs. In the top contact structure, the organic semiconductor is deposited on top of the gate dielectric layer. Source and drain electrodes are then patterned on top of the organic semiconductor layer by shadow masking. The shadow masking technique greatly simplifies source-drain patterning and circumvents the use of time-consuming, more complex patterning techniques such as photolithography. In the bottom contact structure, the source and drain electrodes are first defined prior to organic semiconductor deposition. The channel lengths created using shadow masking are typically greater than 25 μm and hence are unsuitable for fabricating fast circuits. In order to achieve the performance required for practical electronics, shorter channel lengths of the order of less than 10 μm are required.

From the point of view of fabrication in practical terms, the bottom-contact configuration is favored over the top-contact structure since conventional lithography or other forms of patterning can be easily carried out on bottom contact configurations without having to expose the active organic material to solvents and chemicals. The trade-off however, comes on the form of electronic and morphological problems at the metal-to-semiconductor contact in the bottom contact structure. Metal electrodes can

affect the growth of organic semiconductor films near the contact edges due to surface energy differences. Therefore, the ordering of organic molecules can be irregular near the contact electrodes and this area degrades the performance of the transistor. The influence of the contact becomes considerable as channel lengths of OTFTs become smaller and most studies of bottom contact n-channel OTFTs employ large channel length devices in which problems associated with contact injection are reduced [18,19].

Interface problems can be alleviated using two techniques while implementing bottom-contact structures. One is the use of suitable self assembled monolayers for treating the dielectric and the electrode surfaces and the other is the use of intermediate layers of a conducting polymer such as poly(3,4-ethylenedioxythiophene)/poly(styrene sulfonate) (PEDOT/PSS). The use of self-assembled monolayers (SAM) at the interface between the metal/insulator and the metal/semiconductor results in improved properties by lowering surface energy differences which assist the formation of ordered thin films [20-22]. Some SAM's are also reported to alter metal work functions, facilitating charge injection. The most common agent for passivating hydrophilic inorganic substrates is hexamethyldisilazane (HMDS), which coats the SiO_2 surface with a lower surface energy trimethylsilyl monolayer [23]. Other silane functional groups such as octadecyltrichlorosilane (OTS), octyltrichlorosilane (OTS-8), and phenethyltrichlorosilane are commonly used for treating the dielectric surface. For the treatment of metal electrodes, thiol-based SAM agents such as nitrobenzenethiol (NBT) and octadecanethiol (ODT) are used for modifying the surface energy of gold source and drain electrodes to facilitate charge carrier injection [24-26].

In some specific applications, the gate electrode for organic thin-film transistors can be defined at the last stage so that the structure looks more like the conventional MOSFET structure as opposed to the inverted structures shown earlier. Such a structure is known as the top-gate structure and is shown in Fig.2.2. In this configuration, the metal electrodes do not have direct access to the dielectric interface at which the field induced charge carriers are accumulated. The charge carriers get injected vertically from the top gate electrode to the accumulation layer, move along the interface, and are collected at the drain electrode. A perceivable advantage of implementing such a structure is that the semiconducting layer is inherently passivated by the gate dielectric. The obvious constraint that originates is that the insulating material and semiconductor have to necessarily be inert with respect to each other.

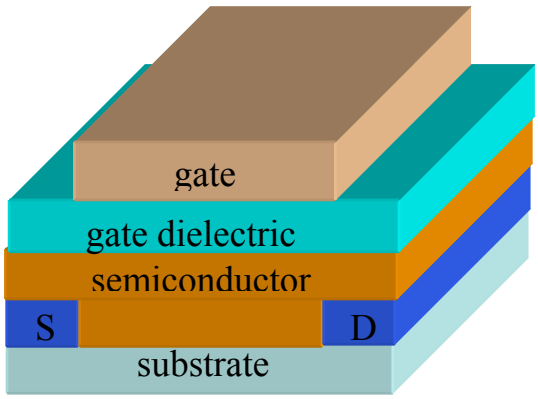

Figure 2.2: Top gate structure for organic transistors.

2.4 Thin-Film Deposition

The most commonly employed techniques for depositing organic semiconductors to fabricate transistors are vacuum evaporation and solution deposition. Vacuum deposited semiconducting layers show good molecular ordering and thin films of oligomers or small molecules such as Pentacene and Copper Phthalocyanine are deposited using this technique. The equipment required for such a system is not entirely cost effective but it gives very good performance due to the ordered nature of thin-films forming the active layer in the transistors. Solution deposition by spin coating, drop casting, ink-jet printing, or stamping is a cost effective alternative to vacuum deposition. This technique is commonly used for polymers. Thin-films of small molecules such as PDI-8CN_2 have also been deposited using solution processing [27, 28].This technique is convenient and promising for low cost, large area applications and mass production of organic devices. It should be noted that the crystalline order of the semiconducting layers achieved using solution processing is inferior to vacuum deposited films. Typical output and transfer characteristics of a Pentacene bottom-contact transistor are shown in Fig. 2.3.

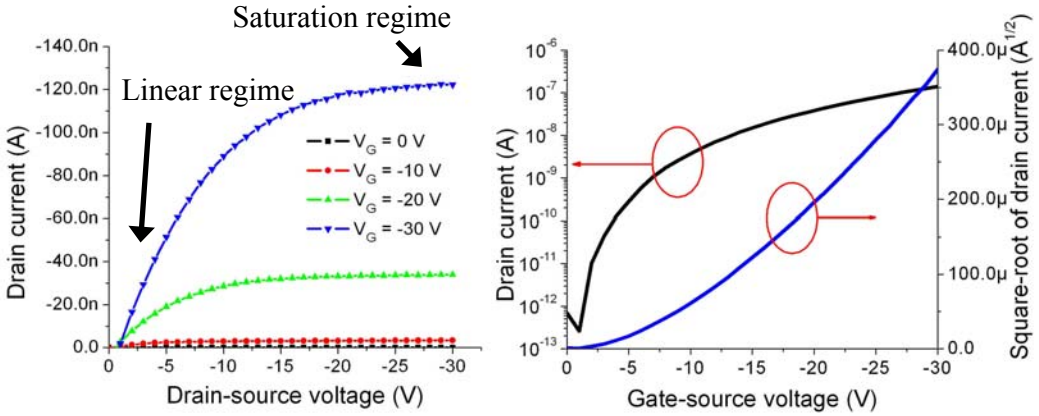

(a) (b)

Figure 2.3: Typical output characteristics (a) and transfer characteristics (b) of a Pentacene OFET [23].

For low values of drain-source voltage, the field created by the gate is uniformly distributed along the channel, giving rise to a uniform distribution of charge carriers. Hence, the drain current is linearly proportional to the applied drain voltage, which forms the linear regime of operations of the transistor. In general, when $0<|V_{DS}|<|V_G-V_T|$, the drain-source current is approximately determined by the standard MOSFET equation [29];

$$I_D = \frac{W\mu C_{ox}}{2L} \times \{2(V_G - V_T)V_{DS} - {V_{DS}}^2\}$$

In the above equation, W is the channel width, L is the channel length, C_{OX} is the capacitance per unit area of the insulating layer, V_T is the threshold voltage, and μ is the field-effect mobility. In the linear regime, the mobility is calculated from the transconductance.

When $|V_{DS}|$ is equal to $|V_{GS}-V_T|$, the electric field created by the gate voltage at the drain contact becomes zero. This is the saturation regime of operation of the OFET wherein additional drain voltage does not induce an increase in the drain current and the drain current is given by;

$$I_D = \frac{W\mu C_{ox}}{2L} \times (V_G - V_T)^2$$

In the saturation regime, the mobility is calculated from the slope of the plot of $|I_D|^{1/2}$ versus V_G as shown in Fig. 2.3(b).

The important characteristics of the device that govern the transport properties of OFETs are the crystalline structure of the organic semiconductor thin-films and the morphology of gate dielectrics. As mentioned earlier, the electrode/semiconductor interface properties determine the injection barrier and the dielectric/semiconductor interface properties affect the molecular ordering within one or two monolayers of the organic semiconductor. The energetics of the system are critical from the point of view of good transistor performance. Interface and inter-grain traps in polycrystalline films also critically affect charge carrier mobility. The effective mobility in polycrystalline materials can be also affected by trapping at grain boundaries [23]. The performance of the transistor and hence circuits fabricated depends on the nature and smoothness of the surfaces involved.

2.5 Organic Transistor Based Circuits

Organic thin-film transistors have a significant advantage over silicon due to low processing costs and due to their compatibility with flexible substrates. P-type OFETs fabricated from small molecules such as pentacene with mobilities in excess of 1 cm^2/V-s have been reported [26, 30]. As already stated, this mobility is orders of magnitude less when compared with the mobilities achieved in silicon. However, the performance of this OFET is very usable in a wide variety of circuit applications. Most OFET circuits implemented now are PMOS circuits.

In the CMOS configuration, p-type and n-type transistors operate in tandem. These systems operate with low static power dissipation and yield high noise margins. Systems in the CMOS configuration can operate at higher speeds as compared to an equivalent p-type circuit. Until recently, most organic circuits were implemented using p-type materials and CMOS had not been widely investigated. This was primarily due to the lack of environmentally robust high-performance n-channel organic semiconductors [31-33].

Many organic transistor based circuits such as inverters, shift-registers and D-Flip Flops have been fabricated using Pentacene and n-type materials such as F_{16}-CuPc, PDI-$8CN_2$ and DFHCO-4T. The inverter is the most simple CMOS circuit to fabricate and can be easily implemented in the top-contact configuration. Other circuits such as the shift register have to be implemented in the bottom contact configuration. The schematic implementation of a top-contact inverter is shown in Figure 2.4. Such a circuit can be

fabricated on a variety of substrates such as a silicon wafer, glass or even flexible polyethylene films. The simplest implementation is with the silicon wafer as it acts as the bottom gate. Silicon dioxide acts as the gate insulator. Selective regions of the wafer are covered for deposition of p-type and n-type organic semiconductors. As shown in the figure, one half of the substrate is deposited with a p-type semiconductor and the other half is deposited with an n-type semiconductor. The source and drain electrodes are so patterned so that there is a common overlapping region that serves as the drain and source electrodes to which supply and ground is connected during testing.

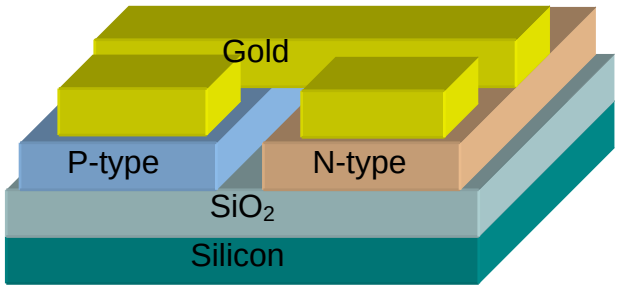

Figure 2.4: Schematic of a top-contact inverter.

The fabrication of circuits such as shift registers and flip-flops is more complex with more number of patterning stages for defining gate contacts and source and drain contacts. These circuits have been implemented and show potential in being integrated with other systems such as microfluidic systems which will be discussed in the following chapters.

2.6 Conclusion

With the development of new air-stable n-type materials, complementary metal oxide semiconductor organic circuits have been fabricated. The fabrication process is not very complex. It is possible to implement such circuits on a variety of substrates. The fabrication and testing of some such circuits and their applicability in serving as drivers for planar microfluidic devices is discussed in Chapter 5. With the aim of this research being the integration of organic transistor based circuits, with microfluidic systems, the following chapters are devoted to giving an overview on microfluidic systems, the design principles involved in the fabrication of these systems, fabrication of organic transistor based circuits and the integration of the two systems. The following chapter gives an overview on microfluidic systems.

2.7 References

[1] Zhenan Bao, Andrew J. Lovinger and Ananth Dodabalapur, Applied Physics Letters, vol. 69, no. 20, 3066 (1996)

[2] H. E. Katz, J. Mater. Chem., vol. 7, no. 3, 369 (1997)

[3] F. Ebisawa, T. Kurokawa, S. Nara, J. Appl. Phys. 54, 3255 (1983)[4] Z.N. Bao, Adv. Mater., 12, 227 (2000)

[5] C.D. Dimitrakopoulos and D.J. Mascaro, IBM J. Res. Dev., 45, 11 (2001)

[6] B. Crone, A. Dodabalapur, A. Gelperin, L. Torsi, H. E. Katz, A. J. Lovinger, and Z. Bao, Appl. Phys. Lett., 78, 2229 (2001)

[7] L. Wang, D. Fine, T. Jung, D. Basu, H. von Seggern, and A. Dodabalapur, Appl. Phys. Lett., 85, 1772 (2004)

[8] C.W. Tang and S. A. VanSlyke, Appl. Phys. Lett., 51, 913 (1987)

[9] P. Peumans, V. Bulovic, and S. R. Forrest, Appl. Phys. Lett., 76, 3855 (2000)

[10] Y. Chen, J. Au, P. Kazlas, A. Ritenour, H. Gates, and M. McCreary, Nature, 423, 136 (2003)

[11] K. Tsukagoshi, J. Tanabe, I. Yagi, K. Shigeto, K. Yanagisawa, Y. Aoyagi, J. Appl. Phys., 99, 064506 (2006)

[12] A. Facchetti, M. Mushrush, H.E. Katz, and T.J. Marks, Adv. Mater., 15, 33 (2003)

[13] M. Halik, H. Klauk, U. Zschieschang, G. Schmid, W. Radlik, and W. Weber, Adv. Mater., 14, 1717 (2002)

[14] H.E.A. Huitema, G.H. Gelinck, J.B.P.H. van der Putten, K.E. Kuijk, C.M. Hart, E. Cantatore, P.T. Herwig, A.J.J.M. van Breemen, and D.M. de Leeuw, Nature, 414, 599 (2002)

[15] N. Koch, J. Ghijsen, A. Elschner, R.L. Johnson, J.-J. Pireaux, J. Schwartz, and A. Kahn, Appl. Phys. Lett., 82, 70 (2003)

[16] M.D. Austin and S.Y. Chou, Appl. Phys. Lett., 81, 4431 (2002)

[17] R. J. Chesterfield, J. C. Mckeen, C. R. Newman, P. C. Ewbank, D. A. da Silva Filho, J. –L. Bredas, L. L. Miller, K. R. Mann, and C. D. Frisbie, J. Phys. Chem. B., 108, 19281 (2004)

[18] S. Kobayashi, T. Takenobu, S. Mori, A. Fujiwara, and Y. Iwasa , Appl. Phys. Lett., 82, 4581 (2003)

[19] S. Kobayashi, T. Nishikawa, T. Takenobu, S. Mori, T. Shimoda, T. Mitani, H. Shimotani, N. Yoshimoto, S. Ogawa, and Y. Iwasa, Nat. Mater., 3, 317 (2004)

[20] A. Salleo, M. L. Chabinyc, M. S. Yang, and R. A. Street, Appl. Phys. Lett., 81, 4383 (2002)

[21] K. P. Pernstich, C. Goldmann, C. Krellner, D. Oberhoff, D. J. Gundlach, and B. Batlogg, Syn. Metals, 146, 325 (2004)

[22] F. F. Fan, J. Yang, L. Cai, D. W. Price, Jr., S. M. Dirk, D. V. Kosynkin, Y. Yao, A. M. Rawtlett, J. M. Tour, and A. J. Bard, J. Am. Chem. Soc., 124, 5550 (2002)

[23] Byungwook Yoo, Applications of molecular electronics to n-channel organic field-effect transistors, complementary circuits, and nanowire transistors, PhD Dissertation (2006)

[24] I. Kymissis, C. D. Dimitrakopoulos and S. Purushothaman, IEEE Trans. Elect. Dev., 48, 1060 (2001)

[25] D. J. Gundlach, L. L. Jia, and T.N. Jackson, IEEE Elect. Dev. Lett., 22, 571 (2001)

[26] S.M. Sze, Physics of semiconductor devices, 2nd Ed., Wiley, New York (1981)

[27] T.W. Lee, Y. Byun, B.W. Koo, I.N. Kang, Y.Y. Lyu, C.H. Lee, L. Pu, and S.Y. Lee, Adv. Mater., 17**,** 2180 (2005)

[28] A. Babel and S. A. Jenekhe, J. Am. Chem. Soc., 125, 13656 (2003)

[29] S.C. Lim, S.H. Kim, J. H. Lee, H. Y. Yu, Y. Park, D. Kim, and T. Zyung, Mater. Sci. Eng. B., 121, 211 (2005)

[30] C. R. Newman, C. D. Frisbie, D. A. da Silva, J. L. Bredas, P. C. Ewbank, and K. R. Mann, Chem. Mater., 16, 4436 (2004)

[31] G.H. Gelinck, H.E.A. Huitema, E. van Veenendaal, E. Cantatore, L. Schrijnemakers, J.B.P.H. van der Putten, T.C.T. Geuns, M. Beenhakkers, J.B. Giesbers, B.-H. Huisman, E.J. Meijer, E.M. Benito, F.J. Touwslager, A.W. Marsman, B.J.E. van Rens, and D.M. de Leeuw, Nature Mater., 3, 106 (2004)

[32] J. Krumm, E. Eckert, W.H. Glauert, A. Ullmann, W. Fix, and W. Clemens, IEEE Elect. Dev. Lett., 25, 399 (2004)

[33] M.G. Kane, J. Campi, M.S. Hammond, F.P. Cuomo, B. Greening, C.D. Sheraw, J.A. Nichols, D.J. Gundlach, J.R. Huang, C.C. Kuo, L. Jia, H. Klauk, and T.N. Jackson, IEEE Elect. Dev. Lett., 21, 534 (2000)

CHAPTER 3 MICROFLUIDIC SYSTEMS

3.1 Introduction

There has been growing interest in the area of microfluidics in the recent years due to the immense potential shown by this field in a wide variety of applications. Microfluidics is the primary thrust for the concept of 'lab-on-a-chip' type systems which involve the systematic integration of complex networks and processes at the micro and nano scale. Microfluidics is the study and analysis of fluids and systems implementing fluidic flows at the micro-scale. There are two main classes of approach to systems incorporating microfluidics, namely continuous flow microfluidics and discrete droplet microfluidics. The conventional approach to microfluidic systems that has been quite actively researched so far has been the continuous microfluidics approach. Such an approach suffers from many shortcomings such as complex fabrication methods and consequently high costs, complicated controls and the use of very high voltages and pressures [1]. Systems employing the continuous microfluidics approach also have fixed or permanently fabricated structures and have restrictions on the liquid being pumped and actuated [2]. These systems also require the use of bulky components such as pumps and valves that have complicated controls. As a result of these inherent constraints associated with the continuous microfluidics approach, such systems are not very convenient for integrating with other electronic and electro-mechanical systems.

Discrete droplet based microfluidics is another approach to handling of liquids at the microscale. This approach for the micromanipulation of unit-sized liquid droplets is also known as digital microfluidics. Such systems tend to be efficient, fairly easy to fabricate and can be integrated with other systems. This is primarily due to the fact that systems implementing such an approach have simple structures that can be reconfigured with great ease. The controls associated with such systems are not complicated either, but typically do require operation at high voltages. The discrete droplet based approach thus gives significant operational advantages over continuous microfluidic schemes. There have been a number of approaches to discrete droplet based systems. Many of these techniques employ the mechanism of electrowetting for the actuation of discrete droplets. Actuation of discrete droplets by using structured surfaces [3], electrochemical principles [4] and thermocapillary effects [5] have been previously investigated. Other methods researched, include dielectrophoretic actuation [6], the use of air pressure [7, 8], and photochemical effects [9]. Reversible red-ox reactions on a conducting polymer surface have also been used to change wetting properties of the surface for droplet manipulation [10]. Electrostatic actuation is a convenient method for actuation of droplets [11] as has been shown by Fair *et al*. in an implementation that does not impose many constraints on the liquid [2]. Discrete droplet based systems are an efficient means to performing basic operations on small volumes of liquids such as moving and mixing of micro- to pico-liter quantities.

An important and integral part of microfluidic devices is the drive circuitry responsible for actuation of the discrete liquid droplets. The drive elements for a number

of implementations have utilized computer controlled voltage sources and other bulky systems such as waveform generators. Gunji *et al*., have demonstrated self-propulsion of water on two parallel electrodes using voltages up to 300 V [12]. Computer based control has been used to generate control signals coupled to the device for micro-particle sampling and mixing of droplets [13, 14]. It would be ideal if there were to be an 'on-chip' drive element to generate the desired voltages for the electrowetting-based actuation of discrete droplets. Such chips, based on Silicon are available, but tend to be expensive. Organic transistor based circuits are a viable option to perform this task, as they are easy to fabricate and can generate the desired magnitudes of voltages required for the actuation of discrete droplets at the micro and nano scale. Large scale complementary circuits based on organic transistors showing a stable and repeatable performance have been previously demonstrated [15]. The voltages and speeds achievable with organic electronics are well matched to the needs of microfluidic devices for the handling of discrete droplets.

This chapter gives a brief outline to primarily two types of implementations of microfluidic systems. The following chapter discusses the actual implementation of a planar discrete device for unit-sized droplet handling. The drive circuitry fabricated to drive the planar microfluidic device is discussed in the subsequent chapter.

3.2 Continuous Flow Microfluidic Systems

Continuous flow microfluidic systems are systems that handle continuous liquid flows. The primary mechanisms for implementation of these types of systems are electro-kinetic techniques, use of mechanical pumps and valves for controlling the quantity and direction of liquid flows, use of pressure variations or by implementing integrated micropumps [16]. These systems perform analyses on different fluid flows that involve continuous flows of liquids in permanently fabricated micro-channels. Due to the nature of these systems in handling flows, the channels that contain the fluids have to be closed structures. A critical drawback of these systems with closed channels is that they are not easily integrated with other systems. The primary reason for this lack of flexibility is that the parameters governing the flow of the fluids in these systems vary along the flow path resulting in the fluid flow in an isolated area of the path critically dependent on the properties of the system as a whole [17]. Fig. 3.1 shows the schematic of an assembly that controls fluid flow in a continuous flow system.

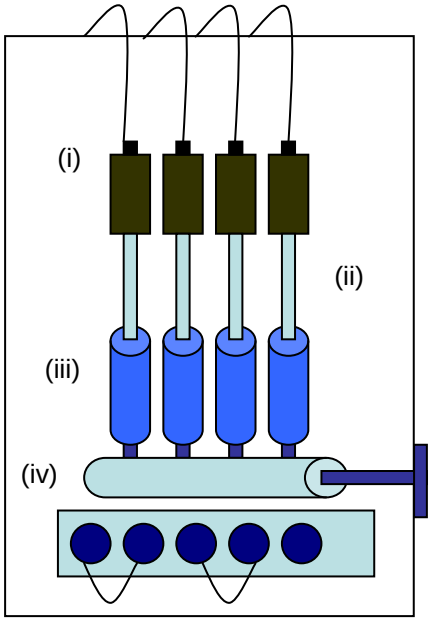

Figure 3.1: This figure shows a schematic of a control unit in a microfluidics system. The components are labeled as (i) flow controllers, (ii) inlets, (iii) liquid reservoirs and (d) control valves adapted from reference [18].

Although these systems work well in applications such as liquid mixing and also in systems that determine conductivity of fluids or pH levels, once fabricated, these systems cannot be reconfigured and are susceptible to breaking down as a whole, even if one working component such as a valve encounters problems. As a result, these systems have poor fault tolerance capability and are unsuitable for tasks that involve complex fluid manipulations [16]. Fig 3.2 shows continuous flow channels in which fluid flows from multiple channels are combined into one composite flow.

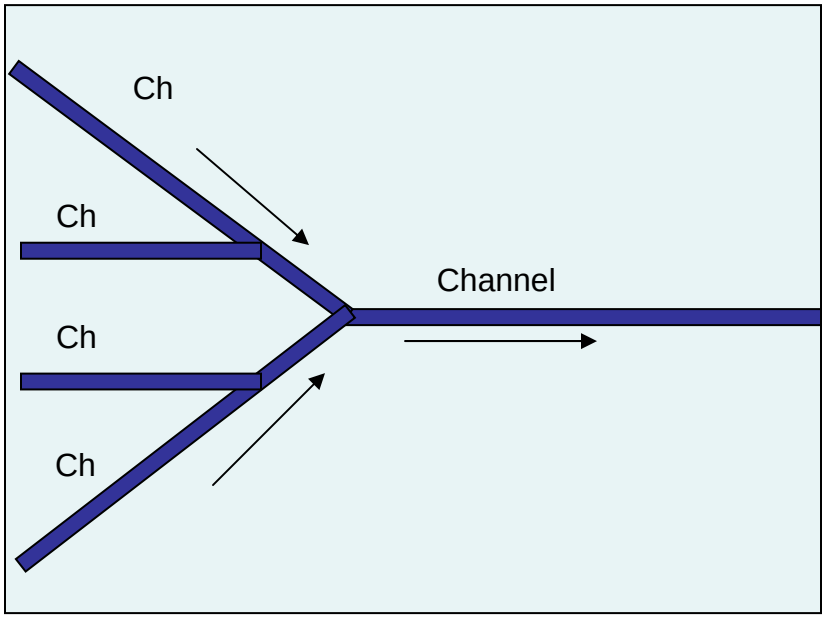

Figure 3.2: This figure shows the schematic of a microfluidic device that is implemented for the formation of continuous flow channels. Adapted from reference [19] (NIST website).

Achieving high levels of functional integration in continuous-flow based microfluidic systems is difficult. Continuous flow microfluidic systems suffer from drawbacks such as complex fabrication methods, complicated controls, high voltage and pressure requirements and large dead volumes of the fluids being pumped in the device [1]. As a result of this, more of recent research has been focusing on the development of discrete-droplet based microfluidic systems. This area of microfluidics is also know as digital microfluidics as it deals with the manipulation of unit or 'digitized' quantities of fluids.

3.3 Discrete Droplet Based Microfluidic Systems

Discrete droplet based microfluidics is another approach to handling of liquids at the microscale. This approach for the micromanipulation of unit-sized liquid droplets is also known as digital microfluidics. Such systems tend to be efficient, fairly easy to fabricate and can be integrated with other systems. This is primarily due to the fact that systems implementing such an approach have simple structures that can be reconfigured with great ease. The controls associated with such systems are not complicated either, but typically do require operation at high voltages. The discrete droplet based approach thus gives significant operational advantages over continuous microfluidic schemes. There have been a number of approaches to discrete droplet based systems. Many of these techniques employ the mechanism of electrowetting for the actuation of discrete droplets.

The implementation of discrete droplet based systems is significantly simpler and it gives a great deal of flexibility. These systems have a scalable architecture and have high fault tolerance capability [16]. As mentioned in the introductory section, there have been a number of approaches to implementing discrete droplet based systems for manipulation of droplets. Using the modulation of surface tension in microscale droplets as the basis for droplet actuation, several techniques are employed in implementing discrete droplet systems [1, 20-22]. Electrowetting is a convenient means to manipulate discrete droplets. Electrowetting is the modulation of the interfacial tension between a liquid in contact with a solid, through an electrostatic mechanism [23- 30]. Such systems are easy to design and implement as the control of electrostatic fields is simple and the

fields are used as the drive mechanism for controlling the movement of droplets. The device geometries required to implement such systems can be easily fabricated. Fig. 3.3 shows electrowetting on application of an electrical potential.

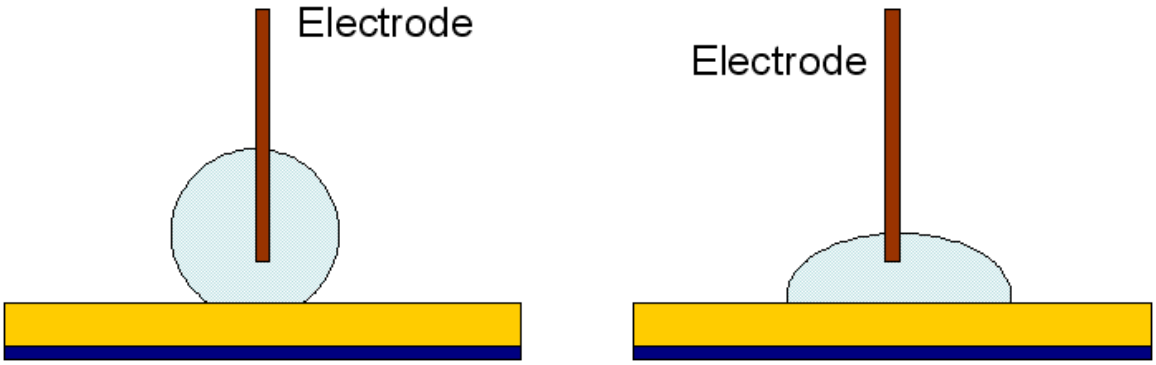

Figure 3.3: Figure shows a droplet resting on an electrode with an insulator. The yellow part is the insulator, and the dark blue region is the substrate. The pin inserted in the droplet is a probe, which is used to apply a voltage that causes a change in interfacial tension between the droplet and the surface causing the droplet to 'wet' the surface better. Adapted from reference [31].

Such a mechanism can be implemented in two ways. In the first structure, the droplet that has to be actuated can rest directly on an electrode to which and electrical potential is applied to. The second geometry introduces another layer on top of the electrode for insulation. This is the addition of a dielectric layer that separates the droplet from the electrode. Such geometry is known as Electrowetting on a Dielectric (EWOD) and is a popular mechanism used as the mechanism for droplet transport in many discrete droplet based microfluidic systems. Another term that is also commonly used for such an implementation is continuous electrowetting (CEW). The EWOD structure is preferred to the structure with no dielectric as there is a possibility of electrolysis of the liquid. This

critically affects the system as the lack of a dielectric layer can limit the strength of the wetting force [32].

Most microfluidic systems that employ the discrete droplet based approach employ the principles of dielectrophoresis and electrocapillarity [33, 34]. These offer a convenient means to control and manipulate discrete quantities of liquids. The governing principle in discrete droplet based systems to achieve basic operations for a functioning Lab on a chip structure is the manipulation of the electro-hydro-dynamic forces that are generated in the presence of an electric field. The mechanism that is employed for the manipulation of droplets is discussed in further detail in Chapter 5 with a focus on the research reported in this dissertation.

3.4 Applications of Microfluidics

Microfluidics has a wide range of applications in various walks of life. The most widely researched application of microfluidic systems is in the area of Lab-on-a-chip systems. There are other applications such as analysis of biological assays, mixing of liquids with different characteristics, conductivity measurements on liquids, particle separation and microfluidic displays [35]. Some other applications of microfluidic systems are in ink-jet printing and in drug delivery/dispensing systems. On a more general level a broad application of microfluidics is in the transport of liquids and various liquid mixtures. Fig. 3.4 and Fig.3.5 show a couple of typical applications of microfluidic systems in mixing and analysis of reagents in a laboratory.

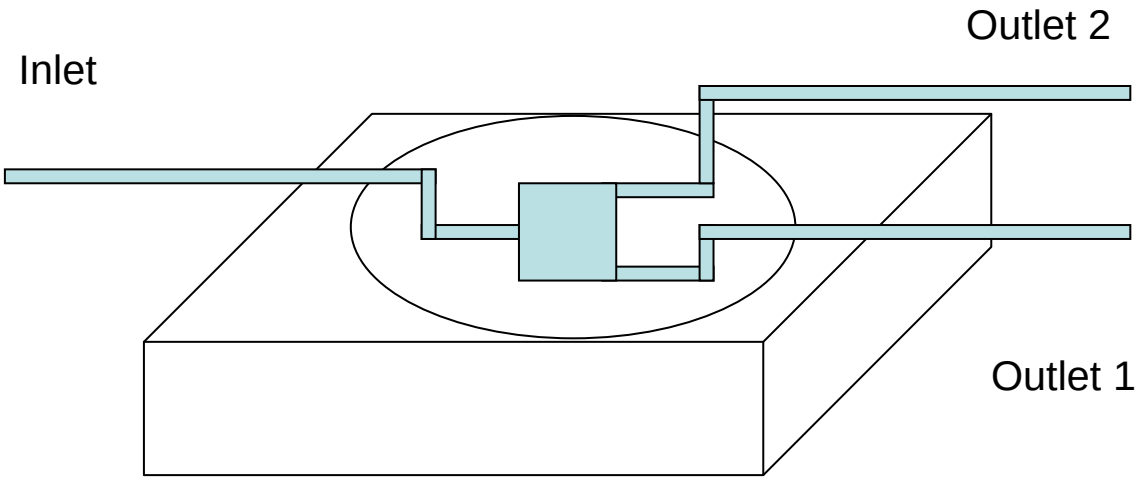

Figure 3.4: Figure shows a bench-top microfluidic system for fluid mixing/particle separation and transport, which can be fabricated with a polymeric material with grooves and inlets, outlet ports through which the test liquids are pumped in and out, adapted from reference [36].

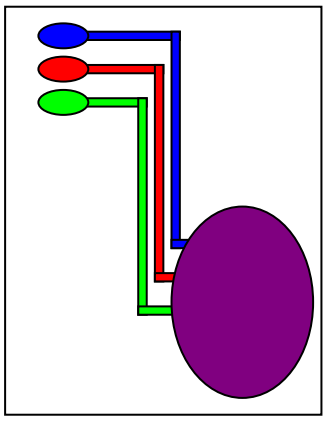

Figure 3.5: This figure shows reagent mixtures being mixed on a single chip with three different inlets containing different liquids being mixed into a reservoir, adapted from reference [37].

The industry that most widely uses microfluidic systems is the bio-medical field. Microfluidic systems have important applications in bio-electro-mechanical systems for the analyses of different types of biological assays, DNA analyses, etc. These systems can form an integrated on chip device for analyzing blood samples, obtaining blood sugar levels and perform various other functions. Microfluidic systems also form an important part of bio-sensors. Some of the potential applications in this area could involve the integration of sensors with a microfluidic system in a self-contained vessel that can be used for performing a number of functions. A futuristic Lab-on-a-Chip drug delivery vessel with a bio-sensor for monitoring blood sugar level in a patient's blood has been portrayed to be part of a smart implant system that can be inserted under human skin in reference [38].

Apart from applications for on-chip laboratories for performing sensing and other functions, microfluidics also finds applications in display devices. There are reports of electrowetting used as the mechanism to modulate the shape of droplet in optical applications such as a tunable lens [29, 39-40]. The implementation of a microfluidic display which can be likened to a Liquid Crystal Display has been shown in reference [41]. There are manufacturing initiatives by some companies like Phillips and Liquavista in Europe that are working on electrowetting based display devices.

3.5 Conclusion

We have thus discussed microfluidics based technology with the two main methods of implementing microfluidic based systems. The chapter compared the design scheme and advantages of using discrete droplet based systems as opposed to taking the continuous-flow microfluidic approach. With most conventional systems hitherto functioning with the continuous flow approach, digital microfluidics is gaining ground as a potent technology for a wide variety of applications. The numerous applications of microfluidics in industry and research have also been discussed. There is much to be learned on the exact mechanics that take place in the functioning of these devices. However, continual progress is being made as the technology evolves. The following chapter deals with the design considerations and implementation of a planar, open-structured microfluidic device for the manipulation of discrete droplets.

3.6 References

[1] M. G. Pollack, A. D. Shenderov and R. Fair, Lab on a Chip, 2, 96 (2002)

[2] Michael G. Pollack, Richard B. Fair and Alexander D. Shenderov, Applied Physics Letters, 77, 11, 1725 (2000)

[3] O. Sandre, L. Gorre-Talini, A. Ajdari, J. Prost, and P. Silberzan, Phys. Rev. E, 60, 2964 (1999)

[4] B. S. Gallardo, V. K. Gupta, F. D. Eagerton, L. I. Jong, V. S. Craig, R. R. Shah, and N. L. Abbott, Science, 283, 57 (1999)

[5] T. S. Sammarco, and M. A. Burns, AIChE Journal, 45, 350 (1999)

[6] T. B. Jones, M. Gunji, M. Washizu and M. J. Feldman, Journal of Applied Physics, 89, 2, 1441 (2001)

[7] Kazuo Hosokawa, Teruo Fujii and Isao Endo, Analytical Chemistry, 71, 4781 (1999)

[8] K. Handique, D.T. Burke, C. H. Mastrangelo, and M. A. Burns, Analytical Chemistry, 73, 1831 (2001)

[9]Kunihiro Ichimura, Sang-Keun Oh, and Masaru Nakagawa, Science, 288, 1624 (2000)

[10] J. Isaksson, N. D. Robinson and M. Berggren, Thin Solid Films, 515, 2003 (2006)

[11] M. Washizu, IEEE Trans. Ind. Applications, 34, 732 (1998)

[12] M. Gunji, and M. Washizu, Jrnl. of Physics D: Appl. Phys., 38, 2417 (2005)

[13] Y.Zhao, and S. K. Cho, Lab on a Chip, 6, 137 (2006)

[14] P. Paik, V. K. Pamula, M. G. Pollack and R. B. Fair, Lab on a Chip, 3, 28 (2003).

[15] B. Crone, A. Dodabalapur, Y.-Y Lin, R. W. Filas, Z. Bao, A. LaDuca, R. Sarpeshkar, H. E. Katz, and W. Li, Nature, 403, 521 (2000)

[16] http://en.wikipedia.org/wiki/Microfluidics referenced from Wikipedia

[17] http://www.answers.com/topic/microfluidics?cat=technology

[18] http://www.cbte.group.shef.ac.uk/research/eng2.html

[19] http://www.eeel.nist.gov/812/MNT/activities.html

[20] K. Handique, D.T. Burke, C. H. Mastrangelo, and M. A. Burns, Analytical Chemistry, 72, 4100 (2000)

[21] M. A. Burns, C. H. Mastrangelo, T. S. Sammarco, F. P. Man, J. R. Webster, B. N. Johnson, B. Foerster, D. Jones, Y. Fields, A. R. Kaiser and D. T. Burke, Proc. Natl. Acad. Sci. U.S.A., 93, 5556 (1996)

[22] J. Lee and C. J. Kim, Journal of Microelectromechanical Systems, 9, 171 (2000)

[23] G. Beni and S. Hackwood, Applied Physics Letters, 38, 207 (1981)

[24] E. Colgate and H. Matsumoto, Journal of Vacuum Science and Technology A, 8, 3625 (1990)

[25] M. Vallet, B. Berge and L. Vovelle, Polymer, 37, 2465 (1996)

[26] H. J. J. Verheijen and M. W. J. Prins, Langmuir, 15, 6616 (1999)

[27] W. J. J. Welters and L. G. J. Fokkink, Langmuir, 14, 1535 (1998)

[28] E. Seyrat and R. A. Hayes, Journal of Applied Physics, 90, 1383 (2001)

[29] C. B. Gorman, H. A. Biebuyck and G. M. Whitesides, Langmuir, 11, 2242 (1995)

[30] V. Peykov, A. Quinn and J. Ralston, Colloid Polym. Sci., 278, 789 (2000)

[31] http://img.clubic.com/photo/012C000000296448.jpg Referenced from the Internet.

[32] H. Moon, S. K. Cho, R. L. Garell and C-J. Kim, Journal of Applied Physics, vol. 92, no. 7, 4080 (2002)

[33] S. K. Cho, H. Moon and C-J. Kim, Journal of Microelectromechanical Systems, vol. 12, no. 1, 70 (2003)

[34] J. A. Schwartz, J. V. Vykoukal and P. R. C. Gascoyne, Lab on a Chip, 4, 11 (2004)

[35] G. Beni and S. Hackwood, Bulletin of the American Physical Society, vol. 26, no. 3, 445 (1981)

[36] http://csrg.ch.pw.edu.pl/tutorials/mTAS/projects.html Referenced from the Internet.

[37] http://www.devicelink.com/ivdt/archive/00/11/0011i47e.jpg Referenced from the Internet.

[38] http://biomechanics.ecs.umass.edu/bioMEMS.jpg Referenced from the Internet.

[39] T. Krupenkin, S. Yang, and P. Mach, Applied Physics Letters 2003, vol. 82, no. 3, 316 (2003)

[40] B. Berge and J. Peseux, Eur. Phys. J. E., 3, 159 (2003)

[41] img.clubic.com/photo/00296453.jpg Referenced from the Internet.

CHAPTER 4: PLANAR MICROFLUIDIC DEVICE IMPLEMENTATION

4.1 Introduction

In Chapter 3, an overview of microfluidic systems has been outlined. As stated, discrete droplet based microfluidics offer significant advantages over continuous flow microfluidic systems in terms of ease of processing and potential for integration with other micro-electro-mechanical systems. It is desired that the microfluidic system that handles discrete quantities of droplets be easy to implement and is cost effective. This chapter discusses various design considerations for the implementation of such a planar microfluidic device. After having discussed these requirements, the implementation of a simple, open-structured, planar microfluidic device is discussed. Two methods of implementation of this device are addressed. The following chapter discusses the integration of this planar device with an organic transistor based circuit.

4.2 Design Considerations

Pioneering work in the area of discrete droplet-based microfluidic systems has been carried out by Richard Fair *et al.*, at Duke University. Up until the early years of this decade, most research had been focused on implementing microfluidic systems that handled large continuously pumped quantities of different liquids for various applications. Most systems of this nature are fabricated on silicon, glass or plastic with

closed channels that do not lend themselves to being reconfigured [1]. The mechanism through which liquids are moved around in these systems include pumping of liquids around the chip using variations in pressure or electrical voltages at isolated locations on the chip, which essentially is the use of electro-kinetic or mechanical means to carry out functions [2-7]. Electrostatic actuation is a convenient method for actuation of droplets as has been shown by Fair *et al* in an implementation that does not impose many constraints on the liquid [8,9].

There are certain standard structures that planar microfluidic devices can be implemented in. These structures are shown in Fig. 4.1.

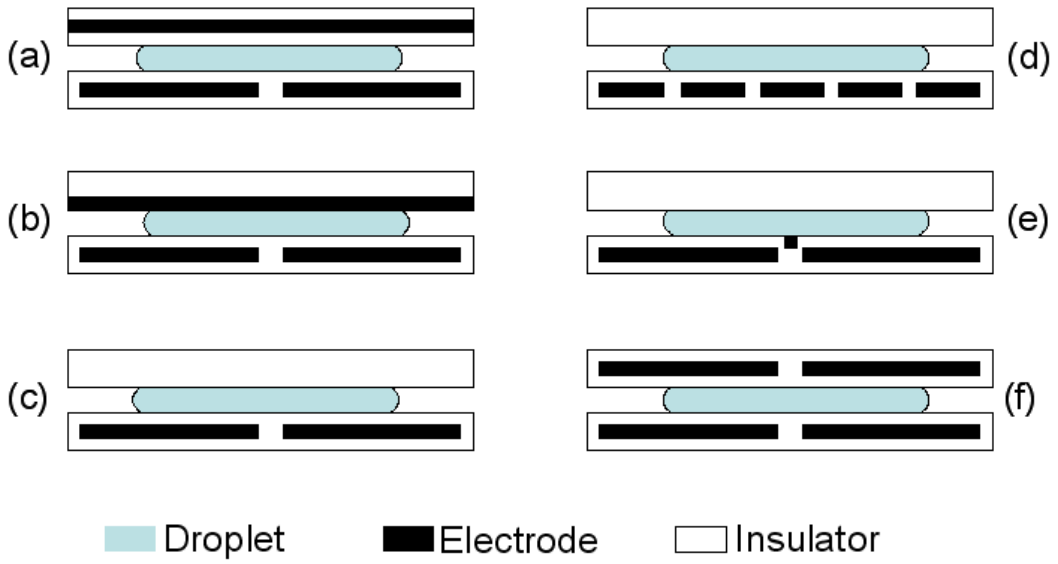

Figure 4.1: Various device configurations for a discrete droplet handling system adapted from reference [1].

These structures use a set of opposing planar electrodes for three dimensional droplet confinement. The variations in the implementations are dependent on the use of an insulator for the top plate, the pitch of the electrodes and the use of an electrode on the top plate. Fig. 4.1 (a) shows the implementation of the device with two sets of opposing electrodes. The bottom plate has an array of independently addressable electrodes with a large pitch. These are coated with a dielectric insulating material. The top plate has one electrode which is also coated with an insulator. The implementation in Fig. 4.1(b) provides no insulating layer for the top electrode. Fig. 4.1(c) shows a top plate with no metal electrode, so the top plate is essentially for confining the liquid droplet. Fig. 4.1(d) is similar to the implementation in Fig. 4.1(c), however, with a smaller pitch of the electrodes. As seen, the droplet resting in between the two opposing electrodes has a footprint that covers more than two adjacent electrodes. Fig. 4.1(e) shows and additional groove electrode on the bottom plate and Fig. 4.1(f) is a symmetric structure that has independently addressable electrodes on both the top and the bottom plates. Thus, there is a significant deal of flexibility in terms of implementing a planar microfluidic device and some geometry can be chosen dependent on the particular application and hence the ease with which a particular geometry can be implemented for a given application. There is also a choice of an ambient fluid that can be used in implementing such structures. The ambient fluid could just as simply be air or it could be an immiscible liquid that surrounds the liquid under consideration such as silicone oil.

As is evident from the various structures shown in Fig. 4.1, there are a number of design considerations that come into play while implementing open-structured planar

microfluidic devices. The critical design considerations for the implementation of a device for handling discrete unit-volumes of fluids are listed below.

(1) Hydrophobicity of the dielectric insulator surface
(2) Stability of the insulator
(3) Magnitude of the applied electrical potential
(4) Pitch of electrodes in the structure
(5) Stability of the surface to carry out reversible wetting
(6) Use of an ambient fluid for confining unit sized droplets of the liquid under consideration

The various design considerations for the implementation of a simple open-structured planar microfluidic device are discussed individually.

4.2.1 Hydrophobicity of the dielectric insulator surface

As discussed in Chapter 3, there are two possible schematics for the implementation of a microfluidic device. The EWOD structure which employs the use of an insulator above a metal electrode is the preferred schematic so that the wetting force on the droplets being manipulated can be maximized. For micro-manipulation of discrete droplets, an extremely hydrophobic surface is essential. Any liquid that under test to be manipulated using a microfluidic device, has to have the ability of not wetting the surface under the presence of no external force such as an electrostatic field. Thus, a smooth

surface with low interface adhesion and friction properties is ideally suited for such systems [10]. There are certain materials that show extreme hydrophobic nature and are rightly called super-hydrophobic materials.

The hydrophobic or hydrophilic nature of a surface is characterized by the contact angle made by a particular liquid when placed on the surface. High surface energy materials like fluorinated polymers have extremely high surface energies that yield high contact angles for droplets such as water droplets. Fig. 4.2 illustrates a hydrophobic and a hydrophilic surface and the difference in contact angles when a droplet is placed on either surface.

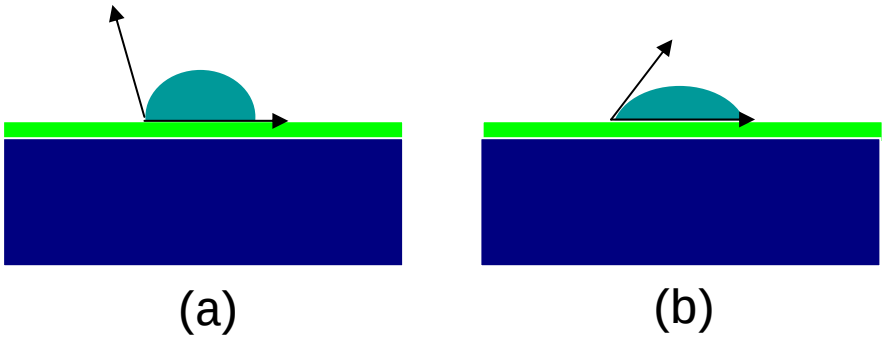

Figure 4.2: figure (a) illustrates a hydrophobic surface which results in a large contact angle as indicated by the arrows and (b) shows a hydrophilic surface in which the liquid resting on the surface wets the surface better resulting in a lower contact angle.

In general, if the contact angle formed by a liquid on a surface is less than 90˚, then the surface is said to be hydrophilic. If the contact angle made by a liquid resting on a surface is in excess of 90˚, then the surface is a hydrophobic surface. There are surfaces that exhibit super-hydrophobic nature. The contact angles for these surfaces are in the range of 150˚ to 180˚.

It is desired that the surface is so selected that the contact angle is maximized for a given system. Electrowetting being the mechanism for manipulation of the liquid droplets, the interfacial tension between the liquid and the solid is altered using an electrostatic potential. Hence, the greater the contact angle modulation that can be achieved on the application of electrostatic charge, the more enhanced is the process of discrete droplet actuation.

In the electrowetting on a dielectric (EWOD) approach, a hydrophobic surface can be created using an insulator that inherently forms a hydrophobic surface or an insulator that does not yield a surface with high surface energy can be functionalized by treating it with some organic material or self-assembled monolayers [11]. Fig. 4.3 shows a droplet of water placed on a wafer of silicon dioxide treated with Hexamethylenedisilazane (HMDS) vapors. Silicon dioxide usually gives a very hydrophilic surface that is completely wetted by water. The HMDS vapors functionalize the silicon dioxide surface making it partially hydrophobic. The contact angle made by the water droplet resting on the functionalized silicon dioxide surface is 81˚.

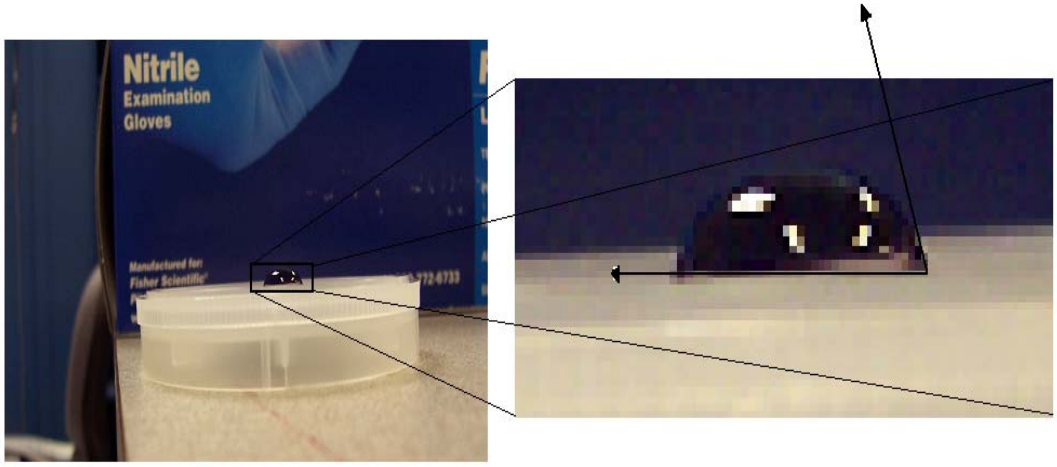

Figure 4.3: Water droplet resting on a silicon dioxide wafer functionalized with HMDS vapors, making the surface partially hydrophobic.

It is desirable to have a material that can result in greater contact angles for liquid droplets resting on its surface. Such a surface can be created using a fluorinated polymer such as Teflon or Cytop. Cytop is an amorphous fluorocarbon, manufactured by Asahi Glass Company and distributed by Bellex International Corp., USA. For similar quantities of water (~ 50µl), a Cytop surface gives a contact angle of 102˚. Fig. 4.4 shows the contact angle made by a water droplet resting on a glass slide coated with Cytop.

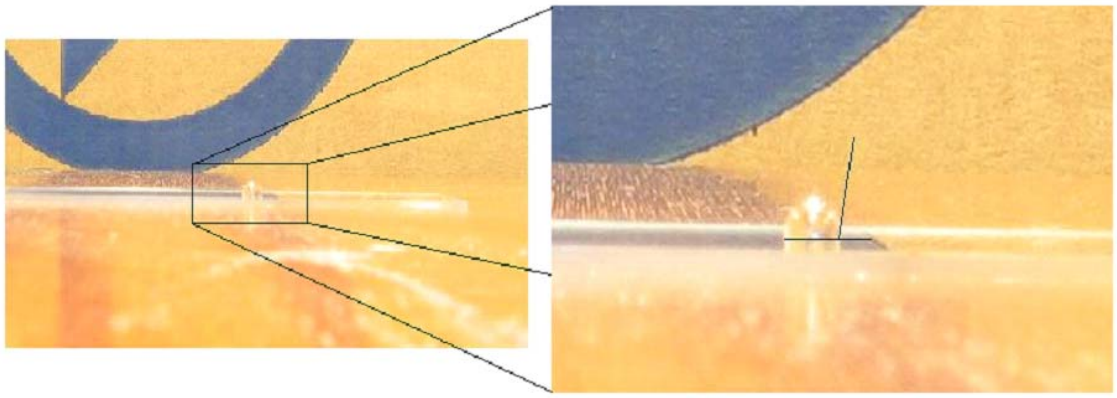

Figure 4.4: Figure shows the high contact angle formed by a water droplet when resting on a Cytop coated surface.

Reversible wetting is a necessary condition for implementing electrowetting based devices. The wetting and de-wetting of a surface can be observed by the contact angle reduction on application of an electric field. It should be noted however, that contact angle reduction is an observable outcome of electrowetting on a dielectric and not necessary for actuation of the droplets [12]. This will be discussed in detail later.

4.2.2 Stability of the insulator

Stability of the insulator or the dielectric material is a critical design consideration while implementing a microfluidic device. The dielectric essentially provides a capacitive coupling between the electrode on which it rests and the droplet that is present on the top surface of the dielectric materials. There is a direct relation between the thickness of the insulator and the magnitude of voltages that are typically used in the actuation of liquid

droplets in such microfluidic schemes. The thinner the thickness of the insulator, the greater is the capacitance. The use of a thicker dielectric allows for the use of greater values of electric potential. The primary consideration for the nature of the dielectric, irrespective of the thickness is its integrity. The insulator isolates the liquid from the metal electrode to prevent electrolysis. However, if there are pin-holes present in the insulator, they act as conduction paths for leakage currents to flow through the dielectric and couple to the liquid droplet under test. This not only causes interaction between the droplet and the applied field resulting in electrolysis, but can also cause degradation in the surface of the dielectric surface. Fig. 4.5 shows the effect of pin-holes present in the dielectric material resulting in a reaction taking place on the insulator surface.

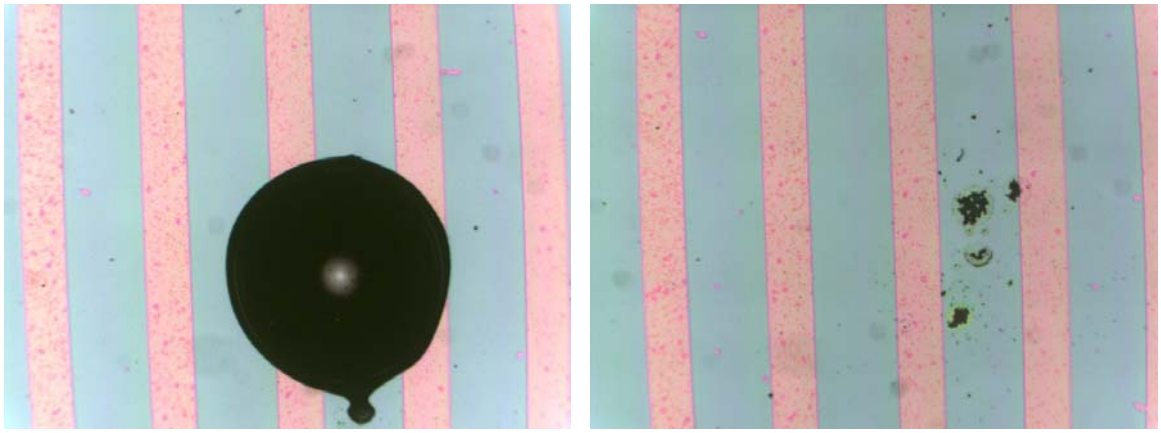

Figure 4.5: Degradation caused from the presence of pin-holes in the dielectric. The left figure indicates the position of the water droplet resting on an electrode. The figure on the right shows the effect of leakage currents on the dielectric surface as a result of interaction with the droplet.

In the photographs shown in Fig. 4.5, the blue regions indicate the metal electrodes and the pink regions indicate the gap between adjacent electrodes. The fabricated device was made on a glass substrate by depositing 1000 Å of Chromium to form an array of independently addressable electrodes. Glass resin was used as the dielectric insulator. It was spin-coated on top of the electrodes to a thickness of 4500 Å. The pitch of the electrodes in this experiment was 800 μm. As can be seen from the figure, glass resin does not perform as a good dielectric insulator. There is a presence of pin holes which result in leakage current coupling to the droplet under test resulting in the electrolysis of the water droplet. The surface of the dielectric was functionalized to make it hydrophobic by treating it with HMDS vapors. The use of voltages in excess of 40 volts caused a degradation of the dielectric surface which is believed to be due to the interaction between the water droplet and the self-assembled monolayers of HMDS caused due to the presence of leakage currents.

The stability of the insulator can be improved by using a bi-layer structure for the dielectric insulator. In our implementations we used a bi-layer structure of glass resin and poly-vinyl-phenol (PVP) to provide for better dielectric strength and alleviate the problems associated with coupling currents through the presence of pin-holes. The trade-off in implementing a bi-layer structure is the increase in the value of electrical potential required to cause the droplet to move from one electrode over to an adjacent electrode. The magnitude of voltages required in implementing a bi-layered structure goes up significantly as compared to the use of a single dielectric insulator with a lesser comparative thickness. Hence, there is a tradeoff between implementing a single-

insulator device and a double-layer insulator device and a particular geometry can be selected as per the requirements of a particular application in terms of flexibility in fabrication, availability of materials and also the magnitudes of voltages that can be generated. This bring us to the next important design consideration for implementing a planar microfluidic device, which is the magnitude of voltages needed to generate sufficient electric filed to actuate discrete droplets.

4.2.3 Magnitude of Electrical Voltage

As mentioned in the earlier section, the thickness of the dielectric insulator has a direct bearing on the magnitudes of electrical voltages that can be applied to the electrodes in a microfluidic device. Usually, this consideration is dictated by the drive circuitry that runs the microfluidic device. If high voltages can be generated with relative ease and the system can be implemented without a lot of complexity then, the use of a thicker dielectric insulator is warranted. Traditionally, the voltage levels used in these systems have been in excess of 100 volts. However, with more research being carried out on various materials lower voltages can be used to actuate discrete droplets in a microfluidic device. A microfluidic device using voltages as low as 15 V has been implemented [13]. In the structures that have been implemented in this research the variation in the applied voltages has ranged from 40 volts to 180 volts. This has been dependent on the nature of the dielectric insulator used as is discussed subsequently in this chapter.

4.2.4 Pitch of the Electrodes

In order to transport independent droplet from one point on the chip to another, a series of gradients in the electrostatic energy have to be generated. Asymmetric electric fields acting on a droplet produce a desired reorganization of charges present at the three phase contact line. The three phase contact line under consideration here is the contact line between the solid, liquid and the ambient fluid. The ambient fluid, dependent on the implementation can be either a gas such as air or it can be an immiscible liquid. The pitch of the electrodes has to be such that an individual droplet when resting on the dielectric surface has a footprint that covers more than two adjacent electrodes. For droplet motion to take place in any one desired direction, there has to be a pressure gradient generated due to the application of an electrical potential. If the pitch of the electrodes is too large, which means the spacing between the electrodes is to wide, the generated electric field will not necessarily cause the motion of the droplets. The accumulation of free charges at the three phase interface gives rise to electro-capillarity [12]. The strength of the wetting force generated at the three interfaces has to be strong enough to act on one edge of the droplet, causing a deformation of the droplet and cause a net motion. On the other hand, a small pitch of electrodes increases the number of points to which an electric charge has to be applied to move the droplet over larger distances. This of course is useful in dealing with smaller sizes of droplets down to the nano scale. However, at such small dimensions, evaporation of droplets becomes and issue and an open structure will not

work. A sandwich structure confining the droplets using a set of opposing planar electrodes has to be implemented.

In the structures implemented in this research, the pitch of the electrodes used is 800 μm. The width of the electrodes is 500 μm with an inter-electrode spacing of 300 μm. Another structure with an electrode pitch of 400 μm was also tested. The earlier device worked well with dispensing droplets with a footprint diameter of ~ 2 mm.

4.2.5 Stability of reaction surface

In typical microfluidic devices using the mechanism of electrowetting on a dielectric, the droplets are in direct contact with the reaction surface. The ambient fluid in these systems is usually air. In systems that employ a dielectrophoretic based actuation mechanism, the droplets being transported are usually surrounded by another fluid that has a higher density. Hence, the droplets being actuated need not necessarily be in contact with the reaction surface. From that point of view, the reaction surface has to be inert and should not be chemically reactive with either the fluid being transported or the surrounding ambient fluid that may be used. Also, the surface on which the droplet actuation takes place has to be such that reversible wetting of liquids can be carried out repeatedly without the degradation of the reaction surface. This is primarily important from the point of view of the lifetimes of such devices. With regard to the reaction surface, it is important to mention that for a longer lasting device, a dielectric insulator

that us fluorinated is preferred over the use of a functionalizing agent to hydrophobize the dielectric surface because such a device is not susceptible to degradation.

4.2.6 Use of ambient fluid

In certain implementations, the droplets being transported are surrounded by an ambient fluid of a different nature, with a higher density. For example, for the transport of water droplets, silicone oil, which is immiscible with water, may be used to facilitate the motion of the droplets by reducing the drag. This type of a structure is typically used in microfluidic systems that employ dielectrophoresis as the mechanism for actuation of droplets. In the EWOD structure, the droplets being actuated are usually confined between two plates; hence, the surrounding media is most commonly air.

4.3 Device Implementation

Having investigated the various design considerations for the implementation of a planar, open-structured microfluidic device, we implemented a simple microfluidic device or the handling and micro-manipulation of discrete droplets of water. The basic structure of the microfluidic device was the same, with two approaches having been adopted for implementing the reaction surface. A schematic of the device fabricated is shown in Fig. 4.6. The fabrication procedure is very simple and devices were fabricated on glass substrates and on silicon wafers.

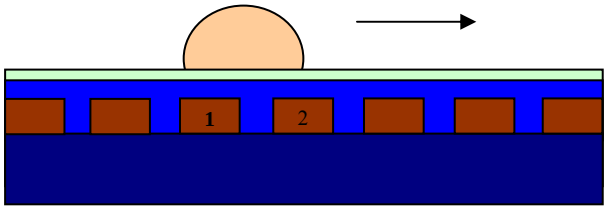

Figure 4.6: Device schematic of the planar microfluidic device. The direction of the arrow indicates the motion of the droplet when electrode 2 is taken to a higher electrostatic potential as compared to electrode 1.

An array of independently addressable electrodes was patterned on a glass substrate in an e-beam metal evaporator using a shadow mask. The use of shadow masks greatly simplifies the fabrication procedure. A schematic of the mask used for patterning the electrodes is shown in Fig. 4.7. The light blue regions indicate the areas in the mask plate that are open so that the metal deposition takes place in those regions.

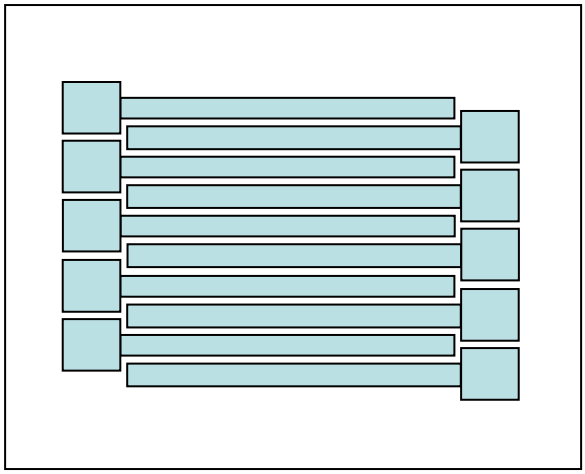

Figure 4.7: Mask design for the patterning of electrodes used for fabricating the array of independently addressable electrodes.

The width of the electrodes is 500 μm with an inter-electrode spacing of 300 μm. The length of the electrode fingers is 2 cm and the electrode pads have a square shape, being 1mm x 1mm in dimensions. The shadow mask was taped onto the glass slide and then placed as the target in the e-beam evaporator for metal deposition. The metal used was Chromium and it was deposited to a thickness of 2000 Å. In an alternative fabrication, Titanium/Gold served as the composite metal for the electrodes with a 30 Å layer of titanium serving as the adhesion layer to 1000 Å of Gold. The dielectric insulator was then deposited on top of the electrodes by spin coating. In initial experiments, glass resin (4500 Å) was used as the dielectric material. The surface of the dielectric was functionalized to make it hydrophobic by subjecting the sample to HMDS vapors. However, this implementation suffered from the drawback of a leaky dielectric. Hence, a bi-layer dielectric insulator structure was then employed using a composite structure of 3000 Å of Poly-vinyl-phenol and 4500 Å of Glass resin. This structure gave stable and repeatable performance as is discussed in the subsequent results section. As stated earlier, the surface of the dielectric insulator was treated with HMDS vapors to make the surface hydrophobic. The voltages required to actuate discrete droplets of water in this implementation were in excess of 80 volts.

In an alternative implementation of the microfluidic device, the bi-layer structure of the microfluidic device was replaced by a single dielectric insulating material that also gave a highly hydrophobic surface. The material used for this implementation was Cytop, which is an amorphous fluorocarbon that forms a good dielectric film and results in a layer that has high surface energy resulting in a contact angle of 102˚ for water droplets

resting on the surface. This structure was also used while driving the microfluidic device using an organic transistor based circuit. This is discussed in the following chapter.

4.4 Results

The two device implementations were tested in the lab using a standard HP 4155 C semiconductor parameter analyzer. It was found that the device with the bi-layer of dielectric insulator exhibited very good breakdown strength. Correspondingly, the voltages required to move droplets over adjacent electrodes were of the order of 80 volts and higher. Changes in contact angle of the droplet were observed for voltages greater than 60 volts. However, actual droplet motion of the water droplets occurred when voltages in excess of 80 volts were applied between adjacent electrodes. Fig. 4.8 shows the motion of a water droplet over adjacent electrodes on the application of a differential voltage of 80 volts.

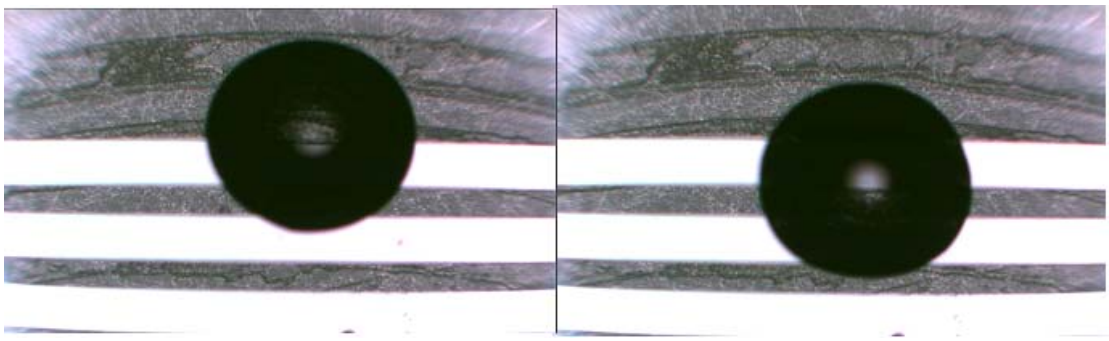

Figure 4.8: Snapshots from a motion camera showing the actuation of a water droplet over adjacent electrodes on the application of an electrical potential. The snapshot on the left is the initial position of the droplet and the snapshot on the right displays the new position of the droplet when the lower electrode on which the droplet partially rested before is energized.

This device worked well over repeated tests and the dielectric material withstood high voltages over multiple runs. The device used HMDS to functionalize the dielectric surface. The self-assembled monolayers of HMDS wear out over time and hence, from the point of view of longevity of the device, this structure is not preferred. The mechanism by which the motion of the droplet takes place is discussed in the following chapter.

The other device which used Cytop as the insulator was also tested under the same testing conditions. Cytop was spun on to the electrodes to a thickness of 4500 Å to form a stable dielectric layer. Multiple tests were carried out on the Cytop surface with water droplets. It was observed that droplet movement took place for voltages in excess of 50 volts. Fig. 4.9 shows the motion of the water droplet over adjacent electrodes on the application of 80 volts.

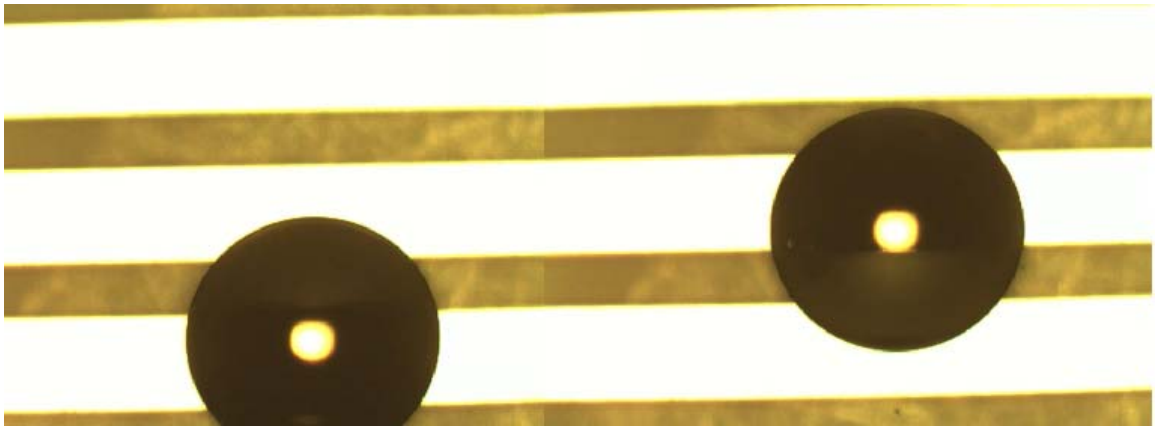

Figure 4.9: Actuation of water droplets over adjacent electrodes on the microfluidic device employing Cytop as the dielectric insulator layer.

The figure shows snapshots of the motion camera Moticam 2000. The frame on the left shows the initial position of the water droplet. It is resting on the lower electrode which is maintained at ground. The droplet partially rests onto the adjacent electrode. When this electrode is energized with respect to the lower electrode droplet movement takes place. The frames show the initial and final position of the water droplet. On observing the videos of the motion recorded by the camera, a change in the contact angle can be seen, which, as mentioned earlier is an observable consequence of electrowetting.

On application of electrical voltage on a series of electrodes one after the other, a water droplet was also shown to move over a range of more than three electrodes. Fig. 4.10 shows three snapshots from the motion camera shown the initial, intermediate and final position of the water droplet when successive electrodes were energized with respect to the previous one, to cause the water droplet to move over three electrodes. The structure implemented in this experiment involved confining the droplet using side grooves that were fabricated using photoresist AZ 5207.

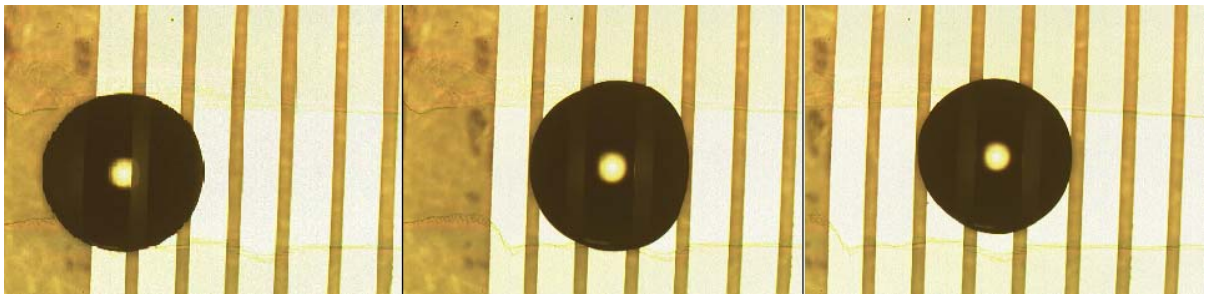

Figure 4.10: Droplet motion over three electrodes. The droplet was laterally confined using grooves that were fabricated using photoresist. Voltages of 80 volts were used to transport the droplet by probing adjacent electrodes in succession.

The fabrication procedure for this device was the same. After depositing the independently addressable electrodes in the E-beam evaporator using shadow masking, photoresist was spun at 4000 r.p.m. for 30 seconds. A single strip in the center of the sample was exposed using photolithography and on developing the sample after exposure, the groove was defined. This was followed by the spin-coating of Cytop. It was found that this structure worked better in moving the water droplet over a series of electrodes. For actuation of the water droplets over adjacent electrodes, the presence of a side groove is not absolutely necessary.

To and fro motion of water droplets was also exhibited on application of AC voltage over adjacent electrodes. In this experiment, the device structure use was the one using Cytop and no groove. Fig. 4.11 displays snapshots from the motion camera showing the initial, intermediate and final positions of the water droplet. A pulsed waveform was generated using a waveform generator and coupled to an amplifier circuit to ramp up the voltage to 100 V.

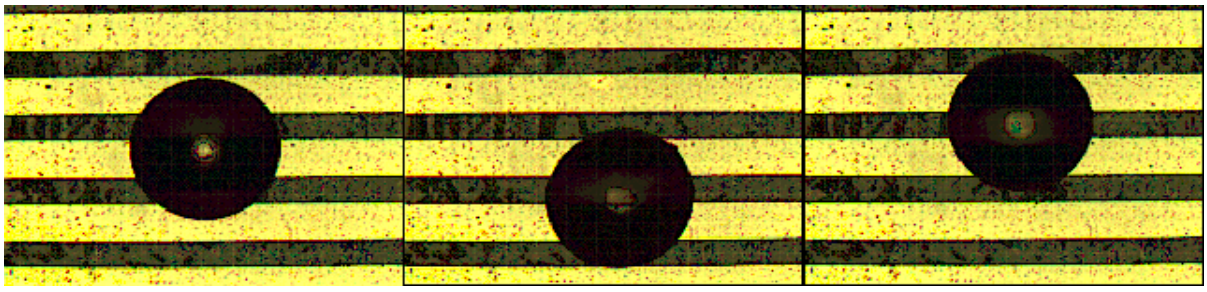

Figure 4.11: To and fro motion of a water droplet on application of pulsed electrical voltages.

As shown in the figure, the droplet is initially at rest such that the footprint of the droplet covers three adjacent electrodes. The droplet covers one electrode on which completely rests and partially over the edges of the two electrodes on either side of the central electrode. The central electrode is grounded and pulsed voltages are applied to both the electrodes on either side of this electrode. The droplet moves to and fro under the influence of the electrostatic field. The pitch of the electrodes and the strength of the field are sufficiently strong to pull the droplet to either side, causing an oscillatory motion. This result is important from the point of view of having the ability for bi-directional motion of the water droplet.

The response of the droplet to application of the electric field is instantaneous. The typical response time in such systems is of the order of microseconds and the voltages are typically in the range of 40 V- 100 V. This makes discrete droplet based devices very suited for being driven by organic transistor based circuits. The results achieved on the open-planar microfluidic device are very promising and this device is integrated with a basic organic transistor based circuit. Other circuits can also be implemented to act as drivers for such systems, for an eventual lab on a chip type implementation with various applications.

4.5 Conclusion

After having discussed the salient features of discrete droplet based microfluidic systems and their advantages over the conventional continuous flow microfluidics counterparts, the design considerations in implementing an open, planar microfluidic device were discussed. There are several design issues that are critical from the point of view of implementing discrete droplet based microfluidic devices. These issues involve the magnitudes of voltages involved in droplet actuation, the nature of the dielectric insulator used, its integrity, pitch of electrodes, nature of the surface and of course the integrity of the surface for repeatable reversible wetting of liquids. A unique microfluidic device has been implemented, which has simple open and planar structure and is easy to fabricate. Droplet actuation was demonstrated over adjacent electrodes. Motion of water droplets over more than two electrodes was also demonstrated using a grooved structure for transporting water droplets. Testing of this structure to confirm to and fro motion of water droplets was also successfully carried out.

The magnitudes of voltages used in the testing of these devices are up to 100 V. The nature and structure of these devices and the levels of voltages involved in driving these devices make them highly suitable for integration with organic transistor based circuits. The suitability and integration of organic transistor based circuits is discussed in the following chapter. Results of implementing an organic transistor based circuit to drive the discrete microfluidic device are discussed and the fabrication and characterization of other organic transistor based circuits is discussed.

4.6 References

[1] M. G. Pollack, A. D. Shenderov and Richard B. Fair, Lab on a Chip, 2, 96 (2002)

[2] A. Manz and H. Becker, Microsystem Technology in Chemistry and Life Sciences, Springer, Berlin, Germany (1998)

[3] P. Gravesen, J. Branebjerg and O. S. Jensen, Journal of Micromechanics and Microengineering, 3, 168 (1993)

[4] M. Elwenspoek, T. S. J. Lammerink, R. Mikaye and J. H. J. Fluitman, Journal of Micromechanics and Microengineering, 4, 227 (1994)

[5] S. Shoji and M. Esahi, Journal of Micromechanics and Microengineering, 4, 157 (1994)

[6] C. H. Mastrangelo, M. A. Burns and D. T. Burke, Proceedings of the IEEE, 86, 1769 (1998)

[7] G. J. M. Bruin, Electrophoresis, 21, 3931 (2000)

[8]M. Washizu, IEEE Trans. Ind. Applications, **34**, 732 (1998)

[9]M. G. Pollack, R. B. Fair, and A. D. Shenderov, Applied Physics Letters, Vol.**77**, No.11, 1725 (2000)

[10] Bharat Bhushan and Yong Chae Jung, Ultramicroscopy, 107, (10-11) 1033 (2007)

[11] S. Nadkarni, and A. Dodabalapur, presented at the 47th Annual TMS Electronic Materials Conference 2005, University of California, Santa Barbara, Session Z (2005)

[12] Jun Zeng and Tom Korsmeyer, Miniaturization for Chemistry, Biology and Bioengineering, Lab Chip, 4, 265 (2004)

[13] H. Moon, S. K. Cho, R. L. Garrell and C-J. Kim, Journal of Applied Physics, vol. 92, no. 7, 4080 (2002)

CHAPTER 5: ORGANIC CIRCUITS AS DRIVERS FOR MICROFLUIDICS

5.1 Introduction

The previous chapter discussed the implementation of an open structured planar microfluidic device. Various design considerations were taken into account before optimizing the device geometry and fabrication. Results of droplet motion were discussed and it was shown that discrete water droplets can be actuated over adjacent electrodes as well as over a series of electrodes. To and fro motion was also exhibited on the application of a pulsed waveform.

For the testing of the microfluidic device, the HP 4155 C standard semiconductor parameter analyzer was used. The independently addressable electrodes were accessed using probes and the necessary voltages for droplet actuation were generated using a waveform generator and a signal amplifier. These systems formed the drive circuitry for the microfluidic device. As mentioned in earlier Chapter 3, an important and integral part of microfluidic devices is the drive circuitry responsible for actuation of the discrete liquid droplets. The most commonly used machinery to drive microfluidic devices has involved the use of waveform generators and computer controlled voltage sources. These sources do generate desired voltage levels for implementation of the device, but are bulky and add a fair level of complexity to the entire system. With the main thrust of microfluidics being a lab on a chip system that performs several functions on an integrated structure, the implementation of an ‘on-chip’

drive circuit to generate the desired voltage levels is highly desirable. Using conventional chips available in the market, it is possible to have a portable source for generating voltages necessary to drive discrete droplet based systems. The inherent limitation with these chips is their cost.

Chapter 2 briefly discussed organic transistor based circuits. The primary advantage in employing organic electronics is the ease of fabrication and cost efficiency coupled with the capability of fabricating these circuits on a variety of substrates. The ability of these circuits to generate high voltages which are well suited to drive discrete droplet based systems make them an ideal alternative for serving as drivers. A lot of research has been carried out on large scale complementary organic transistor based circuits [1-5]. Complementary circuits perform better than their p-type counterparts in better noise margins and lower static power dissipation.

This chapter discusses the fabrication and testing of some organic transistor based circuits such as a CMOS inverter, D flip-flop and ring oscillator. The circuits have been fabricated using Pentacene as the p-type semiconductor and PDI8CN_2 (N,N'-bis(n-octyl)-dicyanoperylene-3,4:9,10-bis(dicarboximide)) as the n-type semiconductor. The results and characteristics of these circuits are discussed. A top-contact inverter is implemented as the driver for the discrete droplet microfluidic device that has been discussed in Chapter 4. Experiments with droplet motion and merging using the top-contact inverter as the drive circuit are discussed and the principle behind the actuation of the discrete water droplets is also explained.

5.2 Materials used in Fabrication

Complementary metal oxide circuits involve the use of both p-type and n-type materials. In the circuits fabricated in our studies Pentacene was used as the p-type material and N,N'-bis(n-octyl)-dicyanoperylene-3,4:9,10-bis(dicarboximide))PDI-8CN_2 was used as the n-type material.

Pentacene exhibits many favorable properties required of semiconductors and has shown charge carrier mobilities good mobilities [6]. Microscopic mobilities of organic molecular crystals fall between 1 $cm^2V^{-1}s^{-1}$ and 10 $cm^2V^{-1}s^{-1}$ [8]. These values are determined by the time-of-flight (TOF) technique [6]. Of all the p-type organic semiconductors investigated, Pentacene has shown the highest mobilities in the above range. Pentacene is a small-molecule polycyclic aromatic hydrocarbon with a strong tendency to form molecular crystals [8], [9]. Pentacene, as a result of this property forms well-ordered films when deposited by thermal evaporation on a variety of substrates [9].

Among the n-type semiconductors investigated, one of the most promising semiconducting materials is *N,N'*-bis(n-octyl)-dicyanoperylene-3,4:9,10-bis(dicarboximide) (PDI-8CN_2), which is a perylene derivative with the -cyano group. This material is synthesized by Prof. Marks / Wasielewski groups at the Northwestern University. The -cyano group increases solubility by decreasing molecular planarity and stabilizes charge carriers by lowering the energies of the lowest unoccupied molecular orbital associated with electron transport [10]. PDI-8CN_2 is an air-stable, robust n-type material that has given very high charge carrier mobilities of up to 0.14 cm^2/ V-s [4].

The substrate used in the fabrication of the CMOS circuits was Silicon. The gate dielectric used in the fabrication of the top-contact inverter was Silicon Dioxide. In the fabrication of other circuits such as the D flip-flop and the shift register, a composite bi-layer gate dielectric of silicon dioxide and silicon nitride was implemented.

5.3 Top Contact Inverter

Top-contact organic transistors generally show a superior performance in comparison with bottom-contact devices. An inverter is a device that toggles between two output states, namely a high state and a low state which is determined by the output voltage levels. The top-contact inverter is implemented using a p-channel FET and an n-channel FET. The input is given to the gate of both these devices in common. The drains of the both FETs are connected together and form the output terminal. The supply voltage is connected with the source of p-channel FET as V_{DD}, and the source of n-channel FET is grounded. When the input voltage is zero, the p-channel FET turns on, and the n-channel FET turns off. Alternatively, the p-channel FET is off and the n-channel FET is on when the applied input voltage is high. Both the devices are connected in series, so that the drain current is ideally zero except the switching time. Only a small charging current flows during the switching operation, thus ensuring that the power dissipation is lesser in comparison with a PMOS inverter. The schematic of a complementary inverter is shown in Fig. 5.1(a).

Lightly doped Silicon served as the bottom gate for the device, 2000 Å of SiO_2 being the gate insulator. Prior to the deposition of the organic semiconductors, the SiO_2/Si sample was treated with Hexamethyldisilazane (HMDS) vapor to improve adhesion and grain ordering of the semiconductor molecules. Dielectric surfaces can be suitably treated to improve the performance of thin-film transistors [11]. PDI-$8CN_2$ was thermally evaporated on one half of the substrate, to a thickness of 350 Å with the substrate temperature at 100˚C, at a deposition rate of 0.5 Å/s. Transistors made from PDI-$8CN_2$ are suitable for fabrication of CMOS circuits as has been reported recently by Yoo et al. [4] Pentacene was deposited on the other half to a thickness of 350 Å with the substrate temperature at 60˚C, at a deposition rate of 0.7 Å/s. There is no overlap between the two films and a glass slide was used to cover either side during semiconductor evaporation. Gold electrodes were deposited to a thickness of 600 Å using shadow masking in an e-beam evaporator. The schematic structure of the top-contact inverter is shown in Fig. 5.1 (b).

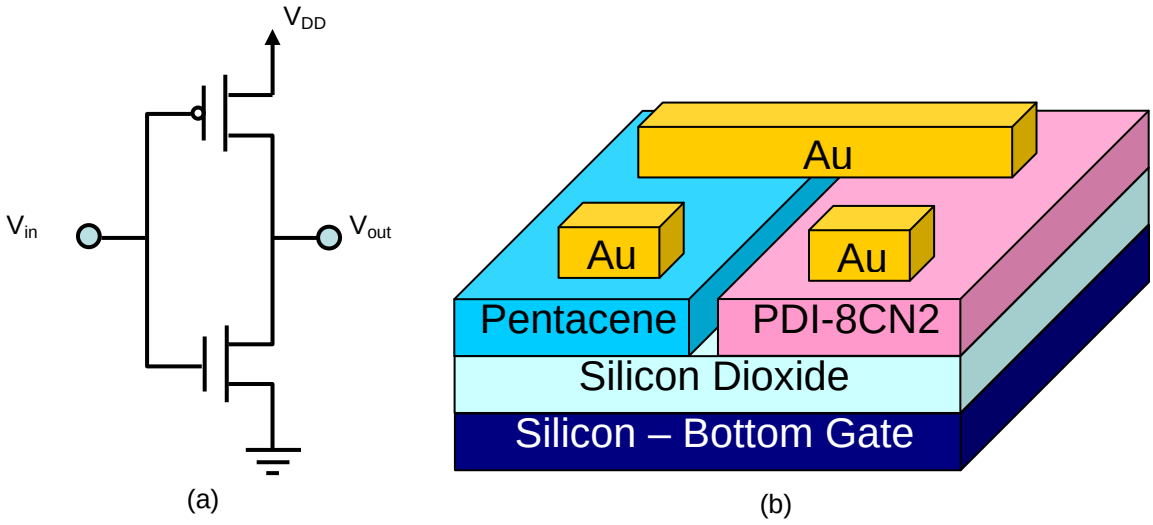

Figure 5.1: The figure on the right shows the device schematic of an inverter and figure (b) shows the schematic diagram of the top-contact inverter fabricated using Pentacene and PDI-8CN_2.

5.3.1 Inverter Results

The top contact inverter was tested for its switching characteristics using the HP 4155 C, standard semiconductor parameter analyzer. The transfer characteristics of the inverter were measured for different values of V_{DD} ranging from 40 volts up to 100 volts. It was found that good switching characteristics were displayed by the top-contact inverter for supply voltages greater than 50 volts. For lower values of voltages, the characteristics are not so reliable. This could be attributable to the fact that the mobilities of the component n-type and p-type materials are not matched. Also, the nature of the materials and exposure to air can result in variations in the threshold voltages of the

transistors. Fig. 5.2 shows the inverter transfer characteristics for a supply voltage of 100 V.

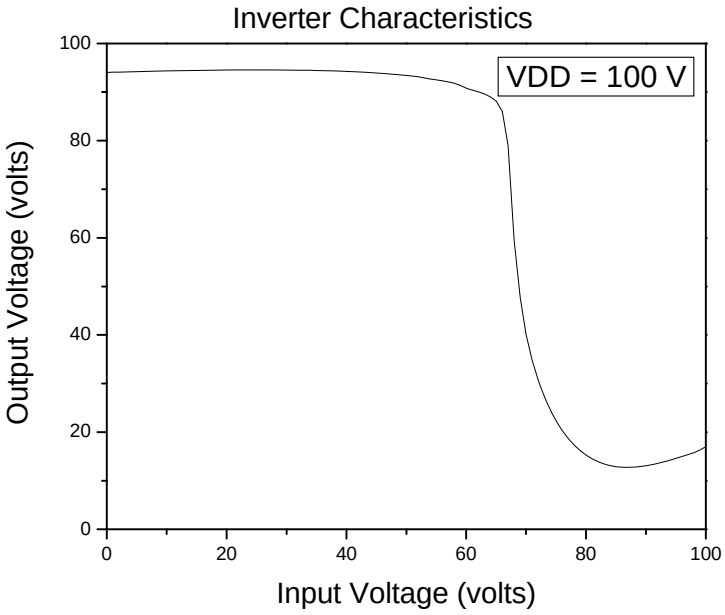

Figure 5.2: Inverter transfer characteristics for V_{DD} of 100 V, and input voltage swept from 0 V to 100 V.

Fig. 5.3 and fig. 5.4 show the transfer characteristics of the top-contact inverter for supply voltages of 60 volts and 50 volts respectively.

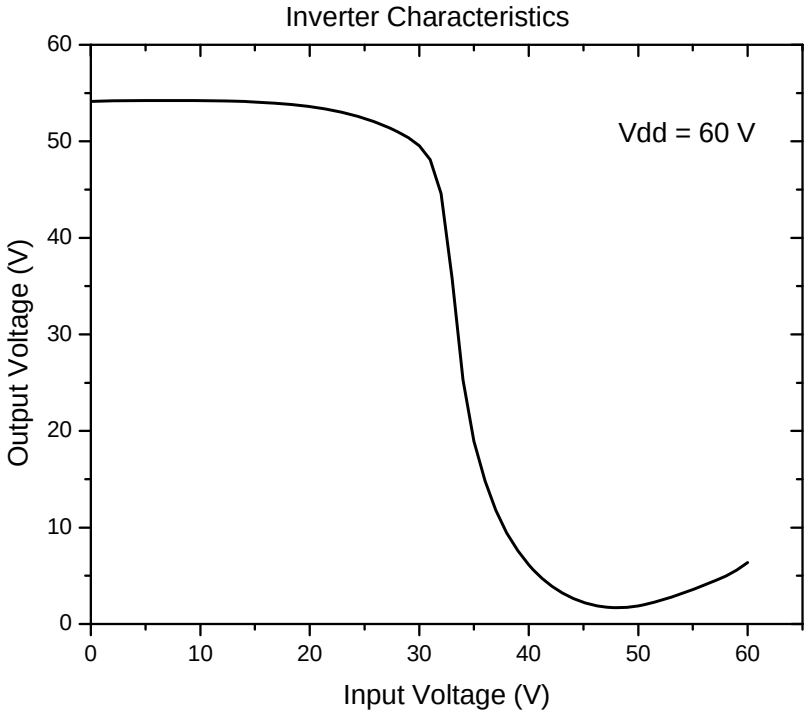

Figure 5.3: Inverter transfer characteristics for a supply voltage of 60 volts.

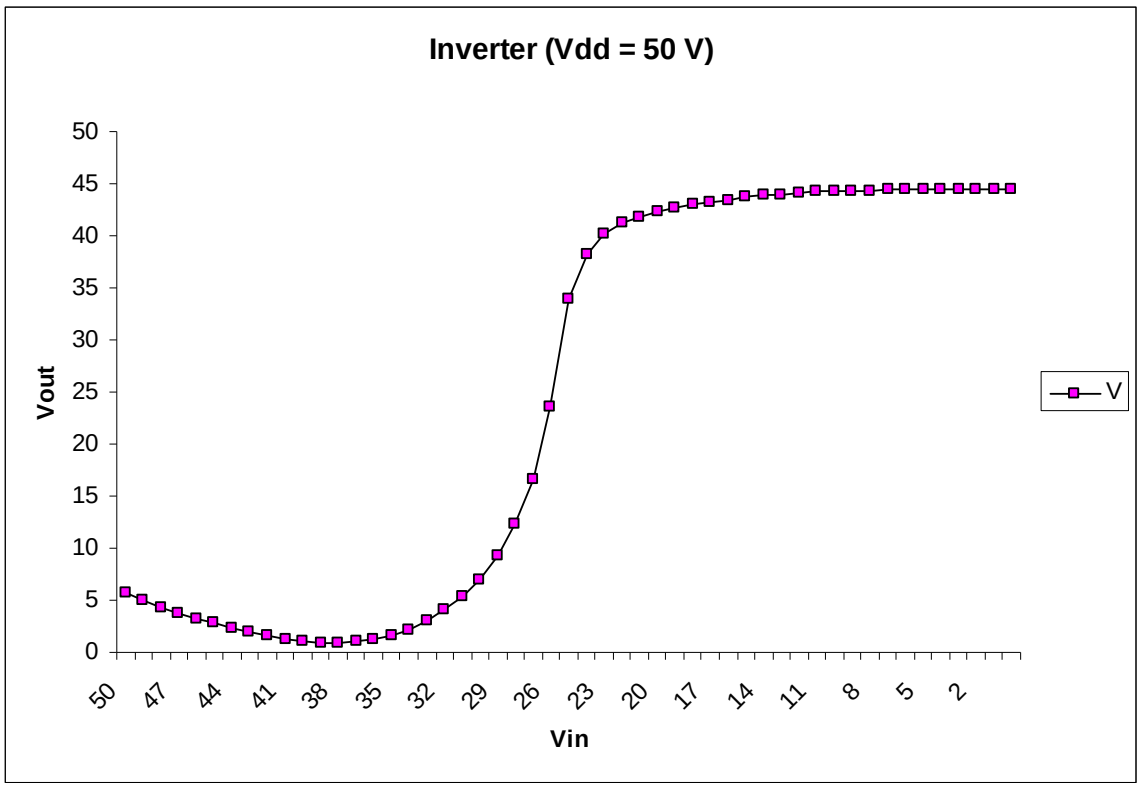

Figure 5.4: Transfer characteristics of the inverter for a supply voltage of 50 volts. The individual data points are plotted for the input voltage variation.

5.4 Other Circuits

The top-contact inverter is the most basic and easy to implement complementary metal oxide semiconductor circuit. The fabrication does not involve any gate patterning and the silicon wafer on which the fabrication is carried out acts as the bottom gate for the inverter. However, for implementation of more complex circuits, the fabrication process is more complex. A schematic of the transistor structure used in the fabrication of other CMOS circuits such as a ring oscillator and a D flip-flop is shown in Fig. 5.5.

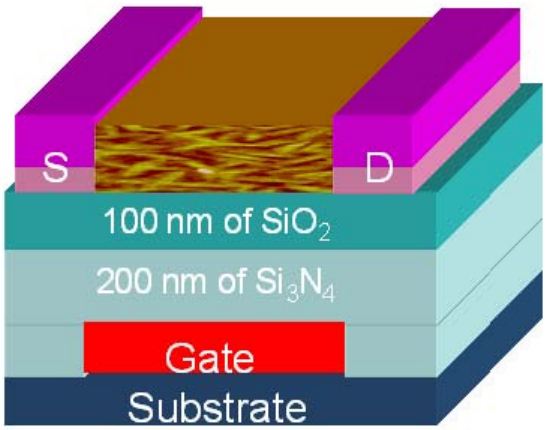

Figure 5.5: Schematic of the transistor structure used in the implementation of CMOS organic circuits.

Bottom-contact discrete transistors were fabricated on silicon substrates. The metal used for interconnects was aluminum. A bilayer of dielectrics, consisting of 200 nm of silicon nitride and 100 nm of silicon oxide served as the gate dielectric. These were fabricated in similar fashion as has been previously reported [12]. The channel width and channel length of the individual transistors are 2.0 mm and 7.5 μm, respectively.

5.4.1 Ring Oscillator

A ring oscillator is formed by connecting an odd number of inverters in a loop and is used in clock generation circuits. Each inverter triggers the next inverter in a cascade connection, and the inverter which is last in the cascade, in turn, triggers the first inverter. A sustained oscillation is achieved due to the fact that the number of inverters in the implementation is odd. The schematic of a five-stage ring oscillator is shown in Fig. 5.6. The operating frequency of the ring oscillator is an indicator of the maximum speed at which the digital circuits can be used.

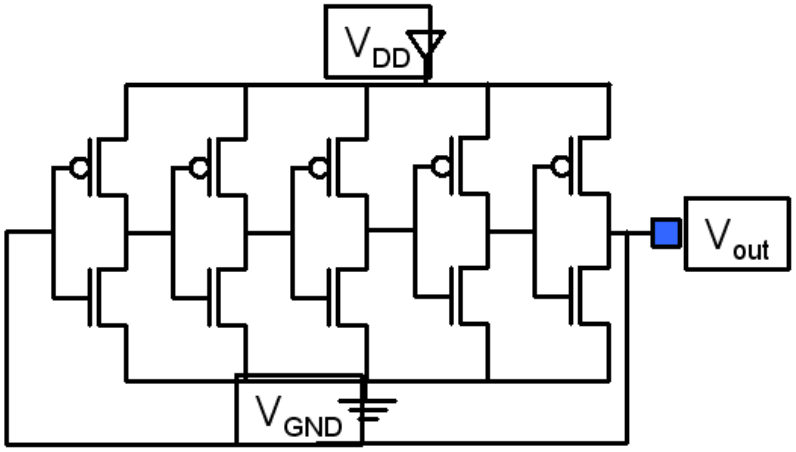

Figure 5.6: Schematic diagram of a five stage ring oscillator.

In the fabrication of the ring oscillator, bottom contact structures were used. Prior to the deposition of the p-type and n-type materials, surface treatments were performed on the sample to improve the nature of the organic thin films as well as improve the injection from the contacts. HMDS vapors served to treat the dielectric surface and 1-hexadecanethiol (HDT) was used in treating the electrodes. The sample was exposed to HMDS vapors in a closed jar for 14 hours. For the HDT treatment, the samples were kept in HDT vapor for 20 min at 135 °C in nitrogen ambient and cleaned with ethanol. Purified Pentacene was thermally evaporated to a thickness of 42 nm with the substrate temperature at 60°C. The electrical characterization was carried out under the vacuum (~1 mTorr) at 300 K with an Agilent 4155C semiconductor parameter analyzer. An Oscilloscope (LeCroy 6030) was used to evaluate the output characteristics of the ring oscillator.

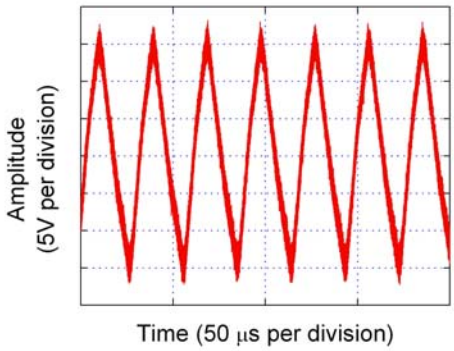

Figure 5.7: Five stage ring oscillator operating at 34 kHz with a supply voltage of V = 100 V [4]. Reprinted with permission from Byungwook Yoo, *et. al.*, Appl. Phys. Lett. 88, 082104 (2006). Copyright 2006, American Institute of Physics.

Fig. 5.7 shows the oscillation frequency characteristics of the ring oscillator with a supply voltage of 100 V. An oscillation frequency of 34 kHz was achieved with a propagation delay (t_p) per stage of ~3 μs [13]. In general, the ring with a certain odd number of inverters (N) will oscillate with the period of $2Nt_p$. The operational frequency of the ring oscillator can be improved by increasing the mobility of n-channel further and by reducing channel lengths and overlap capacitances between the source/drain electrodes and the gate.

5.4.2 D flip-flop

A D flip-flop is a basic storage element in constructing sequential logic circuits and systems. The schematic diagram of a conventional master-slave D flip-flop is illustrated in Fig. 5.8. The pass-transistor logic based D flip-flop requires 16 transistors

which is less than the transistors required for NOR/NAND based logic. The D flip-flop is usually composed of two latches and each latch consists of two CMOS transmission gates and two inverters. When the clock (Clk) is low, the input data D passes directly to the node Q'. Since the clock bar is high at the same time, node Q' is separated from the output node Q, and the feedback loop is closed so that the slave latch is in the storage state. The input data are sent to the slave latch when the clock is high. Therefore, the output starts to collect at the node Q when the input data D is at logic 1 and the clock converts from logic 0 to 1.

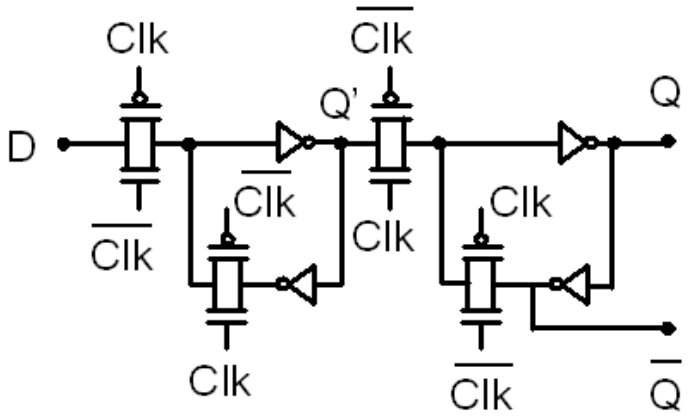

Figure 5.8: Master-slave D flip-flop schematic diagram.

The structure of the transistors used was similar to the structure of the transistors used in the fabrication of the ring oscillator. Surface treatments of HMDS and HDT were performed on the wafer prior to the deposition of the semiconductors. The n-

type semiconductor PDI-8CN_2 was purified by sublimation and thermally deposited onto the substrate held at 100 °C, to a thickness of 42 nm. The Pentacene film (42 nm) was deposited at a substrate temperature of 60 °C. The base pressure was 4×10^{-7} Torr and the deposition rate was 0.2-0.7 Å/s for these depositions. The electrical characterization of the fabricated circuit was conducted in ambient atmosphere at room temperature.

For testing, 100 V of V_{DD} and 0 V of V_{GND} were supplied from a standard Agilent 4155C semiconductor parameter analyzer to the sample. A Tektronix AWG 2005 arbitrary waveform generator was used to create the clock and clock bar signals. These signals were amplified to 100 V by an Avtech amplifier before being supplied to the sample. The system was also triggered from the arbitrary waveform generator by 5 V of trigger signal and amplified to 100 V by HP 214B pulse generator. The position of this pulse was set at the rising edge of the clock pulse. These input signals were monitored on a LeCroy 6030 oscilloscope.

The fabricated D flip-flop was simulated using the T-SPICE program, using models and procedures similar to those described in [12].The measured and simulated characteristics for a pass transistor logic based D flip-flop at a clock frequency of 1 kHz are shown in Fig. 5.9 (a). The black line, blue line, green line, and red line represent the measured output, simulated output, data signal, and clock signal, respectively. The speed of this D flip-flop is limited by one transmission gate and one inverter delay after the clock switches from logic 0 to 1. Fig. 5.9 (b) shows the measured and simulated characteristics at a clock frequency of 5 kHz. It was observed that the measured output started to degrade [13]. The output still follows the clock and data signal.

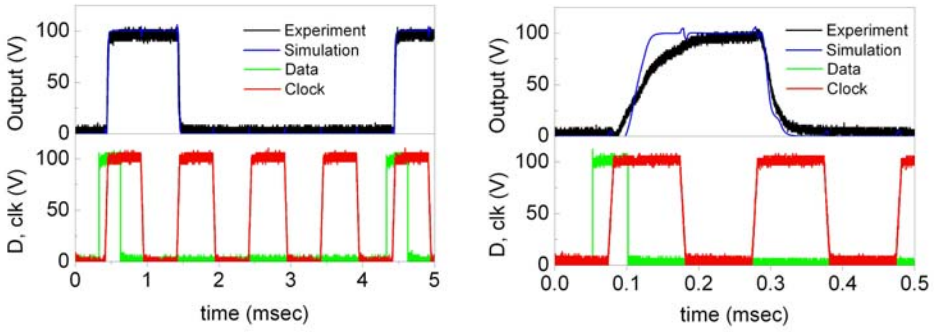

Figure 5.9: The figure shows measured output (black line), simulated output (blue line), data signal (green line) and clock signal (red line) of the D flip-flop at (a) 1 kHz and (b) 5 kHz. Reprinted with permission from Byungwook Yoo, *et. al.*, IEEE Elect. Dev. Lett. 27, 737 (2006). Copyright 2006, IEEE.

5.5 CMOS Inverter as Driver for Microfluidic Devices

Various circuits were implemented using top contact and bottom contact geometries. The circuits fabricated are capable of generating voltages that are necessary to drive discrete droplet based microfluidic systems. The top contact inverter has been used as the driver for the actuation of discrete water droplets on the planar microfluidic device. The inverter generates voltage levels that provide for the necessary electrostatic energy required to move discrete, unit sized quantities of droplets. The results achieved using the top-contact inverter as a driver for the planar microfluidic device is discussed.

As discussed in Chapter 4, voltages in the range of 40 V to 100 V are required for the actuation of discrete droplets on the planar microfluidic device. The output voltage from the top contact inverter was given to an independently addressable electrode on the planar microfluidic device. The schematic for the setup is shown in Fig. 5.10.

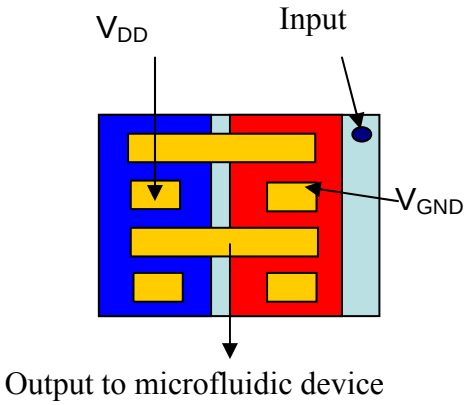

Figure 5.10: Figure shows the setup for connecting the inverter output to the planar microfluidic device.

The inverter was used to drive micro-liter quantities of water droplets over adjacent electrodes. The size of the droplets used in the experiments measures 1.9 mm in diameter, large enough so that the footprint of the droplet spanned more than two adjacent electrodes. Fig. 5.11 shows three frames taken from the motion camera used to capture the motion of the droplet. A Moticam 2000 motion camera was used to track and record the motion of the droplet.

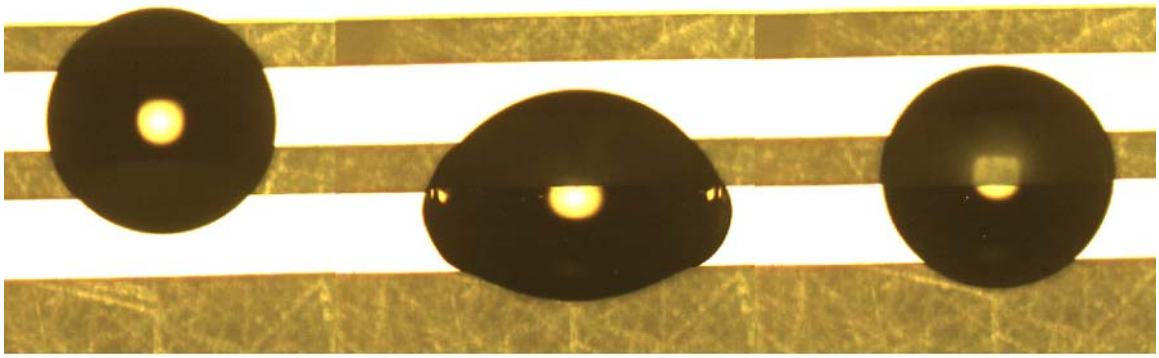

Figure 5.11: Droplet actuation on application of the inverter output [14].

The droplet is initially at rest such that it covers more than one adjacent electrode. The electrode on which it is resting is maintained at ground and the output of the inverter is given to the adjacent electrode, on which the droplet partially rests. As shown in Fig. 5.10, the droplet is initially at rest. On applying the inverter output to the lower electrode, the droplet gets asymmetrically deformed and a resulting motion to the energized electrode is seen. The output voltage of the inverter in this case was 100 V.

Droplet merging is a basic operation in lab on a chip type system performing microfluidic functions. Merging of two droplets over adjacent electrodes was also shown on application of the inverter output [15]. Fig. 5.12 shows stills from the motion video capturing the motion of two droplets from opposing directions, merging to form on aggregate.

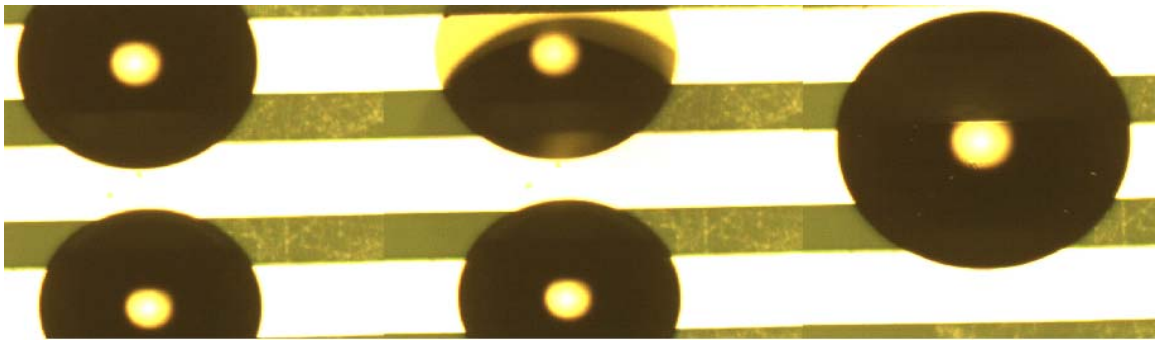

Figure 5.12: Droplet merging on application of the inverter output. Reprinted with permission from Suvid Nadkarni, *et. al.*, Appl. Phys. Lett. 89, 184105 (2006). Copyright 2006, American Institute of Physics.

Inverter outputs for lower values of supply voltages were also applied to the microfluidic device. Droplet motion was observed for lower values of voltages down to 50 volts. For voltages up to 50 volts, there is no bulk movement of the droplet in the direction of the energized electrode. However, the droplet does spread and wet the surface better on application of the inverter output. This can be observed by the change in contact angle that results from the application of the inverter output to an electrode. Droplets were moved in forward and backward directions by coupling the inverter output to the microfluidic device. It is observed that for lower values of voltages, the motion of the droplet is sluggish as compared to its motion when the magnitude of the applied voltage is higher. The response is more rapid and the bulk motion is instantaneous for voltages of the order of 70- 100 volts. It should be noted that the magnitude of the applied voltage that can drive a discrete droplet is also critically dependent on the thickness of the dielectric insulator. Fig. 5.13 shows the motion of the water droplet when the inverter

output is coupled to the microfluidic device. The supply voltage to the inverter in this case is 50 volts.

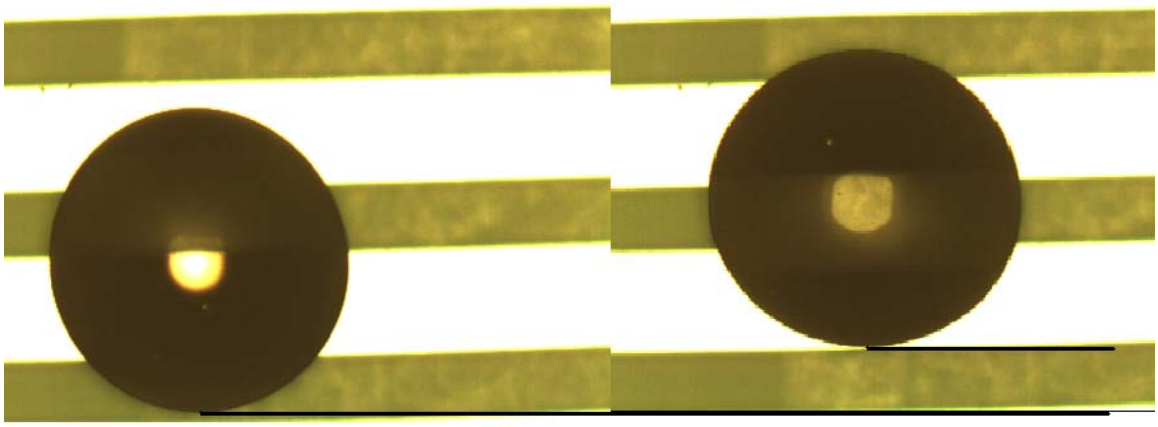

Figure 5.13: Figure shows the snapshots of the initial position of the droplet on the left and the final position on the right on application of the inverter output. The distance traversed is indicated by dark lines.

In Fig. 5.13, the broader white bars indicate the electrodes that are 500 µm wide and the dark bars indicate the inter-electrode spacing which is 300 µm. For actuating the droplet, the bottom electrode is maintained at ground and the inverter output is applied to the upper electrode as shown in the figure. The bottom electrode is the one that the droplet completely rests on in its initial position. The droplet only partially covers the adjacent electrode.

Fig. 5.14 shows the motion of a water droplet over adjacent electrodes on application of the inverter output, when the supply voltage being given to the inverter is 60 volts. The footprint of the droplet used in this case is lesser than the size of the droplet

in previous cases. The droplet diameter in this case is ~ 1 mm and the distance traversed by the droplet is ~ 300 μm.

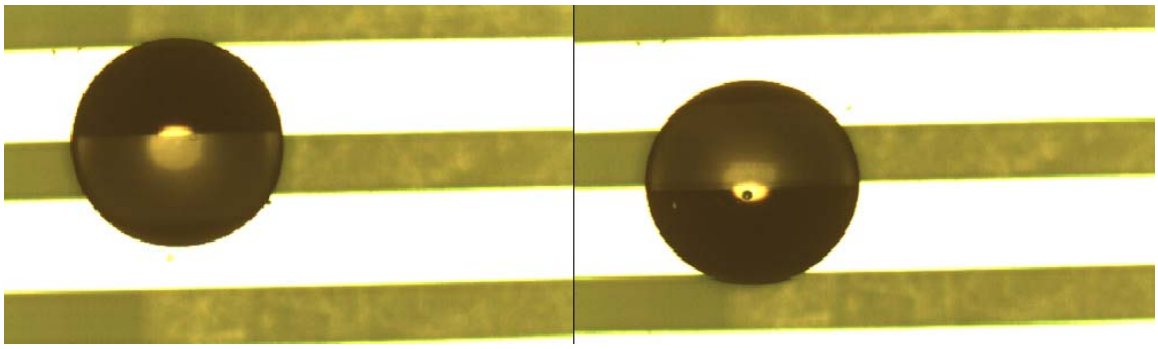

Figure 5.14: Droplet movement over adjacent electrodes for a supply voltage of 60 volts applied to the inverter.

There was no observed dependence of the distance traversed by the droplet and its size. As mentioned before, the response of the droplet is much quicker when the magnitude of the applied voltage goes up. The motion of the droplet is dependent on the magnitude of the applied voltage and the thickness of the dielectric insulator. For thinner insulator thicknesses, droplets can be actuated by the application of lower values of voltages. The mechanism behind the actuation of the water droplets is known as electro-wetting which means the modulation of the wetting property of a liquid on a solid by application of electrostatic energy. The surface tension of discrete droplets is modulated based on the re-ordering of charges present at the three-phase interface. The principle of operation is discussed in the following section.

5.6 Mechanism of Droplet Actuation

In discrete droplet based systems for lab-on-a-chip architectures, the basic set of operations such as droplet transport and droplet merging is carried out by generating electrohydrodynamic forces through the application of an asymmetric electric field. As in most structures as well as the planar open-structured microfluidic device discussed in this research, an independently addressable electrode array is utilized to generate the forces necessary for droplet actuation in a predetermined fashion. In most systems, the forces operate on multiple phases. In the system implemented in our experiments, we work with three phases namely solid, liquid and gas. There are two primary mechanisms which are employed for the generation of electrohydrodynamic forces in discrete droplet based systems, namely electro-capillarity and dielectrophoresis [16, 17].

There are several device configurations in systems that employ electro-capillarity as the mechanism for droplet actuation. Dependent on the way in which the systems are implemented, the mechanism is referred to as electrowetting, continuous electrowetting or electrowetting on a dielectric. The most commonly used configuration in the implementation of lab-on-a-chip type systems is the electrowetting on a dielectric (EWOD) configuration. The system works on the principle of creating a non-uniform interfacial tension at the interface to two media resulting in a bulk motion that causes the movement of droplets.

Dielectrophoresis is another mechanism that is commonly employed as the operating principle for lab-on-a-chip architectures. Dielectrophoresis is the phenomenon

that results in electromechanical forces being exerted on a particle that is electrically neutral, on exposure to an electric field [18]. Dielectrophoresis originates from the property of a particular medium like an insulator, to get polarized. This differs from electro-capillarity, wherein the primary driving force is the accumulation of free charges at the interfaces [18]. In either case though, the presence of multiple media is the basic requirement for operating discrete droplet based systems.

5.6.1 EWOD and Dielectrophoresis [18]

Electrowetting on a dielectric and dielecptrophoresis are the most commonly employed and strong mechanisms for the actuation of discrete fluid droplets. A wetting force induced by the presence of an electric field is completely or partially responsible for the movement of discrete droplets. In the EWOD configuration, the electric energy gives rise to the wetting force and this force is responsible for the movement of the droplets. On the other hand, in the dielectrophoretic mechanism, the contributions that result in the motion of the droplets are not only from the wetting force, but also from force acting at the interface of the two fluids, force acting on the tri-phase contact line and a body force which is manifested in the form of a gradient in pressure.

Most EWOD configurations employ two plates, an upper plate and a lower plate to encapsulate the droplet being transported. The ambient fluid is usually air and it is necessary that the droplet is in contact with the plates. On the other hand, in typical implementations of dielectrophoretic chips, the droplet being transported is surrounded

by another immiscible liquid. The fluid being actuated rests on top of the immiscible fluid and it is not necessary for the droplet to make contact with the reaction surface as is required in EWOD implementations. In effect, the presence of free charge at the interfaces in a three phase system give rise to electro-capillarity, which is electrowetting on a dielectric and dielectrophoresis, arises from the polarizability of the media present in the system.

5.6.2 System under Consideration

In the planar open-structured microfluidic device that has been the platform for actuating discrete water droplets in this research, there is no presence of a top plate with a dielectric insulator. The ambient fluid in all experimentation is air and the droplets being actuated are always in contact with the reaction surface. Due to the nature of the system implemented in this research the exact mechanism that causes the actuation of water droplet is due to a combination of forces that are acting on the interfaces of the three media, namely, solid, liquid and air.

For the given thickness of the insulator used in experiments, voltages in excess of 50 volts were required to actuate droplets over adjacent electrodes. For voltages up to 50 V, there is no bulk motion of the droplet, but there is an observable change in the contact angle on the side of the electrode to which the electrical voltage is applied. Fig. 5.15 shows the displacement of the droplet which is observed as an increase in the footprint size of the droplet indicated by ‘Δ’ in the figure. This is effectively an increase in the

wetting of the surface by the droplet and an increase in wetting results in the corresponding reduction in the contact angle made by the droplet with the insulator surface. The figure shows snapshots from the motion camera indicating the droplet footprint before the application of 40 volts (left side) and the footprint after the application of 40 volts (right side). The white lines seen in the snapshots are the electrodes. For this test, the bottom electrode on which the droplet rested was grounded and 40 volts was applied to the adjacent electrode (top electrode seen in the figure).

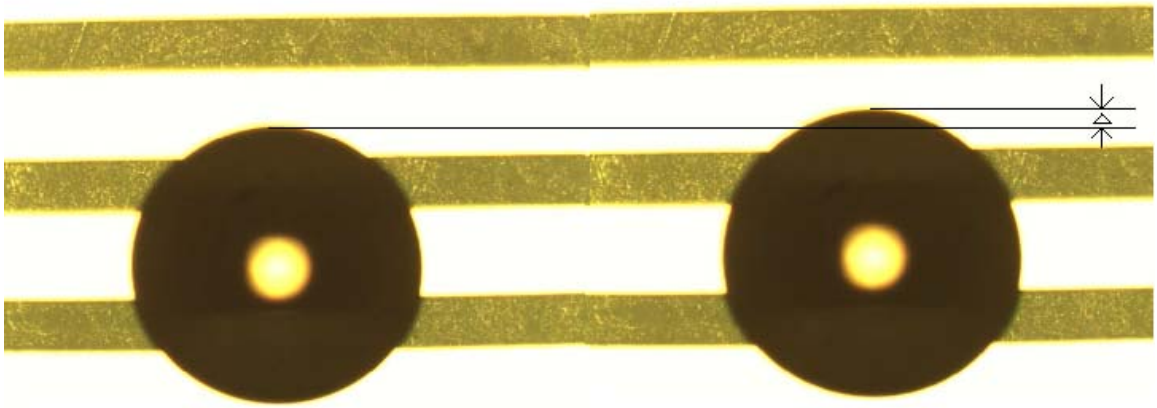

Figure 5.15: Contact angle reduction shown by the increase in droplet footprint when 40 volts is applied to the top electrode with respect to the bottom electrode maintained at ground. The increase in the droplet footprint is indicated by 'Δ'.

If 'Φ' is the contact angle made by the droplet with the surface of a hydrophobic insulator with thickness 't', then the modification in the contact angle occurs per the Young-Laplace equation [19], given by

$$\cos\Phi(V) = \cos\Phi(0) + \frac{\varepsilon_0 \varepsilon_r}{2t\sigma_{LG}} V^2 \qquad (1)$$

where V is the magnitude of the applied voltage, σ_{LG} is the surface tension at the liquid-gas interface; ε_0 is the permittivity of free space and ε_r is the dielectric constant of the insulator. A variable capacitance system is formed by the droplet, the insulator and the electrode [20]. The motion of the droplet, when an electric potential is applied to the electrode, is to maximize the capacitance of the system, thereby reducing the energy [21]. The application of an electrical potential induces an image charge of opposite polarity in the droplet, resulting in a pressure gradient that manifests itself in the form of a reduced contact angle due to a change in the interfacial energy. The solid-liquid interfacial energy 'σ_{SL}' varies with the applied voltage as follows [19]:

$$\sigma_{SL}(V) = \sigma_{SL}(0) - \frac{\varepsilon_0 \varepsilon_r}{2t} V^2 \qquad (2)$$

As can be seen from equations (1) and (2), the thickness of the insulator is critical from the point of view of the device being able to withstand high electrical voltages. For thinner insulators, breakdown would occur earlier. The thickness of the insulator can be varied as per the requirement of the device and the magnitude of the voltages it would be expected to handle without breaking down.

The observed change in contact angle, which is seen from the increase in the droplet footprint on the application of the voltage, indicates the presence of the wetting force. The change in contact angle of the droplet is due to the presence of this wetting force. A spatial variation in the wetting force results due to the fact that the droplet is

resting on one electrode that is grounded and another electrode that is energized to a particular voltage. The wetting force needs to be sufficiently strong for droplet actuation to take place. It is critical to note that motion of the droplet would occur even if the droplet were to be non-deformable [18]. Hence, a change in the contact angle is merely an observable outcome of electrowetting on the dielectric and it stems from the variation in the electro-quasistatic energy present in the insulating layer.

As was observed in the experiments carried out with the planar microfluidic device, for a Cytop thickness of ~ 4500 Å, 50 V was sufficient to generate a wetting necessary for transporting the droplet over adjacent electrodes. Fig. 5.16 shows three still frames from left to right, indicating the initial, intermediate and final position of the water droplet upon application of 50 volts to the electrode adjacent to the grounded electrode, upon which the droplet initially rests. As has been mentioned earlier, the rapidness with which the droplet moves was found to have a dependence on the magnitude of the voltage applied, with a more rapid movement at higher voltages in excess of 70 V. As is seen in the figure, the motion of the droplet is relatively sluggish for the applied 50 V.

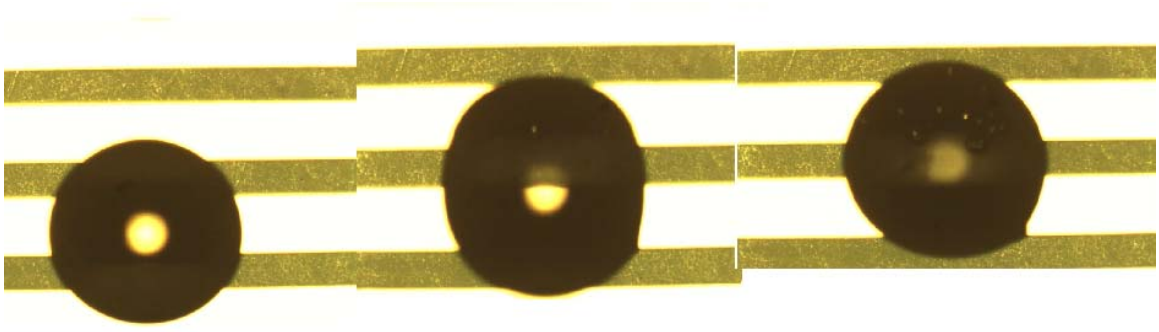

Figure 5.16: Droplet movement on application of 50 V to the top electrode.

From the frames shown in Fig.5.16, it is apparent from the second still frame that the droplet spreads on the application of the voltage. The spreading is more pronounced on the leading edge, which is the edge resting on the electrode to which the voltage is applied. The trailing edge of the droplet, wets the surface slightly lesser than the leading edge due to the fact that the electrode is grounded.

The mechanisms at work in inducing a shear flow in the droplet are the excitation of free charges at the interface of the two fluids and the force acting on the tri-phase contact line. Initially, the flow is generated at the interface between the two fluids. This is the origin for the wetting force that results from the presence of free charge at the interface between air and the insulator and the water droplet and the insulator. There is also a contribution from the polarization charge present due to the inconsistency in stored energy in the insulating layer [18].

We believe that there is a contribution due to a dielectrophoretic mechanism as well. This is observed while carrying out fusion of two droplets. As mentioned in our experiments the ambient fluid is air and not an immiscible fluid that surrounds the droplet. It is known that two droplets approaching each other experience an increase in the electric field as the proximity between the droplets increases [18]. This increase in attraction between the droplets is due to the force acting on the two fluid interface between the water droplet and air.

An important outcome of the research presented in this dissertation is the resolution of contributions from electrowetting forces as well as a dielectrophoretic contribution. In the experiments performed on the water droplet at 100 V to induce to and

fro motion, time delayed pulses were applied over adjacent electrodes (Refer to Figure 4.11). It was found that there is a toggling motion of the droplet over the adjacent electrodes. The droplet initially moves to one electrode. At this point, there is no overlap between the droplet and the top electrode. The fringing fields at the edge of the electrode exert a force at the interface between water and air and draw the droplet towards the top electrode. This is clearly seen in the motion video that captures the motion of the droplet. In the initial move to the lower electrode, the droplet slides to the energized electrode. In the motion back in the direction of the upper electrode, a deformation of the droplet is observed. This is not a deformation similar to an increase in the footprint area. Hence, we conclude that the forces at the interface between the water and air are causing the deformation as opposed to the deformation seen in Figure 5.16 which is as a result of the wetting force acting at the interface of the three media. This is a unique structure that has been implemented and the effects from the presence of an electrowetting force and a dielectrophoretic force are observed.

In summary, the main mechanisms operational in the manipulation of discrete liquid droplets are polarization and conduction, which are the mechanisms at the molecular level that respond to an external electric field [18]. The electric nature of a fluid is characterized by a spatial distribution of free charges and dipole moments [18]. The presence of free charges at the interfaces of different media and a non-uniform distribution of polarizable charge in the solid insulator result in a variable charge distribution induced by an electric field. The reordering of charges that ensues from the application of an external voltage is manifested in the form of a force imbalance on

opposing ends of the water droplet, thus inducing a shear flow. The flow originates at the interface between the droplet and air and propagates into the bulk, causing the droplet to move under the influence of an applied electric field.

5.7 Conclusion

An organic transistor based top-contact inverter has been implemented to act as the driver circuit for the planar microfluidic device. The inverter has been shown to have a stable and repeatable performance in driving discrete droplets over adjacent electrodes as well as in carrying out droplet merging. Other CMOS circuits such as a ring oscillator and a D flip-flop have also been implemented. Organic transistor based circuits are ideal for acting as the drive elements for discrete droplet based microfluidic systems as the compatibility of the two systems from the point of view of required voltages as well as the times scales, is ideal.

The mechanism for droplet actuation has also been discussed with the primary driving force being electro-wetting. However, due to the nature of the system, there are other contributing forces that aid the actuation of the droplet on application of an electric field. The asymmetric nature of the field creates a force imbalance which is due to the accumulation of free charges at the interface between the fluids as well as the polarization of charges in the insulating layer. Net motion of a droplet takes place when a sufficient force imbalance is created in the droplet. We have shown with experimentation, that motion of the water droplets takes place due to electrowetting forces and contributions

from dielectrophoretic forces as well. The contribution from both these mechanisms is resolved for the structure that has been implemented.

We have thus shown that organic transistor based circuits show great potential for integration with discrete droplet based systems, in acting as an on-chip driver circuit. An organic transistor based circuit was successfully used to actuate water droplets over adjacent electrodes and the mechanisms inducing the motion of the droplets were also investigated experimentally.

5.8 References

[1] B. Crone, A. Dodabalapur, Y. –Y. Lin, R. W. Filas, Z. Bao, A. LaDuca, R. Sarpeshkar, H. E. Katz and W. Li, Nature 403 (6769), 521 (2000)

[2] A. Dodabalapur, Materials Today, vol. 9, no. 4, 24 (2006)

[3] M. Kitamura and Y. Arakawa, Applied Physics Letters, 91, 053505 (2007)

[4] B. Yoo, T. Jung, D. Basu, A. Dodabalapur, B. A. Jones, A. Facchetti, M. R. Wasielewski and T. J. Marks, Applied Physics Letters,88, 082104 (2006)

[5] B. Yoo, D. Basu, T. Jung, D. Fine, B. A. Jones, A. Facchetti, M. R. Wasielewski, T. J. Marks, K. Dimmler and A. Dodabalapur, presented at the 64th Annual Device Research Conference (2006)

[6] G. A. de Wijs, C. C. Mattheus, R. A. de Groot and T. T. M. Palstra, Synthetic Metals, 139, 109 (2003)

[7] M. Pope and C.E. Swenberg, Electronic Processes in Organic Crystals and Polymers, 2nd edition, Oxford University Press, New York, 1999, 337-340

[8] Hagen Klauk, David J. Gundlach, Jonathan A. Nichols and Thomas N. Jackson, IEEE Transactions on Electron Devices, vol. 46, no. 6, 1258 (1999)

[9] Y.-Y. Lin, D. J. Gundlach, S. F. Nelson and T. N. Jackson, IEEE Transactions on Electron Devices, vol. 44, no. 8, 1325(1997)

[10] B.A. Jones, M. J. Ahrens, M.-H. Yoon, A. Facchetti, T.J. Marks, and M.R. Wasielewski, Angew. Chem. Int. Ed., 43, 6363 (2004)

[11] A. Salleo, M. L. Chabinyc, M. S. Yang, and R. A. Street, Applied Physics Letters, vol. 81, no. 23, 4383 (2002)

[12] B. K. Crone, A. Dodabalapur, R. Sarpeshkar, R.W. Filas, Y.Y. Lin, Z. Bao, J. H. O'Neill, W. Li, and H.E. Katz, J. Appl. Phys., 89, 5125 (2001)

[13] Byungwook Yoo, Ashwin Madgavkar, Brooks A. Jones, Suvid Nadkarni, Antonio Facchetti, Klaus Dimmler, Michael R. Wasielewski, Tobin J. Marks and Ananth Dodabalapur, IEEE Electron Device Letters, 27, 9, 737 (2006)

[14] Suvid Nadkarni and Ananth Dodabalapur, Journal of Materials Science: Materials in Electronics, 18, 9, 931 (2007)

[15] Suvid Nadkarni, Byungwook Yoo, Debarshi Basu and Ananth Dodabalapur, Applied Physics Letters, 89, 184105 (2006)

[16] S. K. Cho, H. Moon and C.-J. Kim, Journal of Microelectromechanical Systems, 12, 1, 70 (2003)

[17] J. A. Schwartz, J. V. Vykoukal and P. R. C. Gascoyne, Lab Chip, 2, 96 (2002)

[18] Jun Zeng and Tom Korsmeyer, Lab on a Chip, 4, 265 (2004)

[19] M. Vallet, B. Berge and L. Vovelle, Polymer, 37, 12, 2465 (1996)

[20] M. Washizu, IEEE Trans. Ind. Applications, 34, 732 (1998)

[21] M. G. Pollack, A. D. Shenderov and R. Fair, Lab on a Chip, 2, 96 (2002)

CHAPTER 6: CONCLUSION

The objective of this research has been the investigation of the suitability of organic transistor based circuits as drivers for discrete droplet based microfluidic systems. The motivation in carrying out the research has been the integration of two viable technologies for an eventual lab-on-a-chip type system that would have the capability to perform a desired set of functions like sensing. Such a chip would be a self-sufficient chip, with all sub-systems such as the driver circuits, droplet delivery system and the sensing array fabricated onto one portable chip, capable of performing various functions. The obvious advantages of using organic transistor based circuits and discrete droplet microfluidics are the ease in processing and cost efficiency rendered on implementing such systems.

We implemented a planar microfluidic device fabricated on a glass substrate using standard microfabrication techniques. The open structure is easy to fabricate and very simple to reconfigure and test. The methods involved in fabrication of the device involved the use of additive methods such as shadow masking to put down electrodes and spin-coating for putting down the insulating layer. There are a number of design considerations that have to be taken into account for fabricating such a device. The design considerations were discussed and the implemented device was explained in Chapter 4. Two ways of implementing the discrete droplet device were discussed and the superior option was chosen for testing with the organic transistor based circuit.

Various circuits using the complementary metal oxide semiconductor architecture have been fabricated and tested. A few of these circuits were discussed in Chapter 5. CMOS circuits are superior to their p-type counterparts in lower power consumption and giving better noise margins. Ongoing research in the synthesis of new air-stable n-type materials is promising from the point of getting high mobility materials for use in organic transistors and circuits. The effect of surface treatments on the growth of organic thin films was also discussed and it was shown that the performance of devices is greatly enhanced on treating the dielectric surface as well as the contact electrodes with various surface treatments. These were implemented in the fabrication of circuits.

The nature of discrete droplet based systems in terms of the magnitudes of voltages required for their functioning along with the time scales on which they operate make them an ideal fit for integration with organic transistor based circuits. Low-cost, easy to fabricate circuits fabricated using organic semiconducting materials are capable of generating the necessary voltages required for the actuation of discrete droplets. The micro-second time scales that are involved in these systems are also in good agreement with the speeds that organic transistor based circuits can provide.

An organic transistor based CMOS inverter was used as the driver for the planar microfluidic device in the actuation of water droplets. A reliable and repeatable performance of the system was exhibited and water droplets were actuated over adjacent electrodes. Droplet merging, which is a critical function in microfluidic systems was also performed using the inverter as the drive circuit.

Water droplets were actuated over a series of electrodes showing that the droplets can be effectively moved over longer length scales and that to and fro motion of droplets can also be achieved using a pulsed voltage. The device performed well over multiple tests and there was no degradation in the surface properties of the device over repeated tests. With experimentation, the mechanisms that induce motion of the droplets were investigated. Electrowetting on a dielectric and dielectrophoresis are the two most commonly invoked mechanisms in discrete droplet transport. In the structure implemented in this research, we resolved contributions from electrowetting forces as well as dielectrophoretic forces in causing the actuation of water droplets.

Organic transistor based circuits have numerous applications and one of the new applications is explored in this work. The implementation of an organic transistor based circuit acting as a driver for a discrete droplet based device is a step in the direction of realizing the eventual goal of a lab-on-a-chip type system with the drive circuitry and the laboratory all on one chip, performing a set of functions that are required of a particular application.

With the initial work having been carried out in the integration of two highly potent technologies, significant work can be done with regards to making progress in this area of research. The development of more complex circuitry that can act as the driver for actuating liquid droplets over longer length scales is the next stage in achieving the goal of having an on-chip all-organic driver circuit. The behavior of various fluids, when subjected to an electric field, needs to be investigated to have a clear idea of the design requirements that would be needed for an application specific system.

This work opens up a new world of possibilities for the use of organic transistor based circuits in discrete droplet base microfluidic systems. With the initial results showing great promise in terms of having a planar, easy to fabricate microfluidic device, and also successful implementation of an organic transistor based circuit to drive such a discrete droplet based device, it will be only a matter of time before a complete organic transistor based lab-on-a-chip becomes a reality.

BIBLIOGRAPHY

http://en.wikipedia.org/wiki/Plastic referenced from Wikipedia

A.G. MacDiarmid, M. Akhtar, C.K. Chiang, M.J. Cohen, J. Kleppinger, A.J. Heeger, E.J. Louis, J. Milliken, M.J. Moran, D.L. Peebles, and H. Shirakawa, J. Electrochem. Soc., 124, C304 (1977)

H. Shirakawa, E.J. Louis, A. G. MacDiarmid, C. K. Chiang, A. J. Heeger, J. Chem. Soc. Chem. Commun., 16, 578 (1977)

Robert Rotzoll, Siddharth Mohapatra, Viorel Olariu, Robert Wenz, Michelle Grigas, Klaus Dimmler, Oleg Shchekin and Ananth Dodabalapur, Applied Physics Letters 88, 123502 (2006)

Liang Wang, Daniel Fine, Deepak Sharma, Luisa Torsi and Ananth Dodabalapur, Analytical and Bioanalytical Chemistry 384, 310 (2006)

B. Crone, A. Dodabalapur, Y.Y. Lin, R. W. Filas, Z. Bao, A. LaDuca, R. Sarpeshkar, H. E. Katz and W. Li, Nature 403, 521 (2000)

C. J. Brabec, Solar energy materials and solar cells, 83, 273 (2004)

J. H. Burroughes, D. D. C. Bradley, A. R. Brown, R. N. Marks, K. Mackay, R. H. Friend, P. L. Burns and A. B. Holmes, Nature 347, 539 (1990)

Rogers, J.A.; Bao, Z.; Baldwin, K.; Dodabalapur, A.; Crone, B.; Raju, V.R.; Katz, H.E.; Kuck, V.J.; Amundson, K.; Ewing, J.; Drzaic, P. Proc. Nat. Acad. Sci. **98**, 4835-4840 (2001)

J. A. Rogers and Z. Bao, Journal of Polymer Science Part A: Polymer Chemistry 40 (20), 3327 (2002)

J. R. Ostrick, A. Dodabalapur, L. Torsi, A. J. Lovinger, E. W. Kwock, T. M. Miller, M. Galvin, M. Berggren and H. E. Katz, Journal of Applied Physics, 81, 10, 6804 (1997)

C. D. Dimitrakopoulos and P. R. L. Malenfant, Advanced Materials, Vol. 14, No. 2, pp. 99-117 (2002)

Tae Ho Jung, Submicron and nanoscale organic field-effect transistors and circuits, PhD Dissertation (2006)

S. Jeyadev and E.M. Conwell, Phys. Rev. B, 35, 6253 (1987)

E.M. Conwell, H.Y. Choi, and S. Jeyadev, Synth. Metals, 49, 359 (1992)

P.G. Le Comber and W. E. Spear, Phys. Rev. Lett., 25, 509 (1970)

C.D. Dimitrakopoulos, J. Kymissis, S. Purushothaman, D.A. Neumayer, P.R. Duncombe, and R.B. Laibowitz, Adv. Mater., 11, 1372 (1999)

C.D. Dimitrakopoulos, S. Purushothaman, J. Kymissis, A. Callegari, and J.M. Shaw, Science, 283, 822 (1999)

G. Horowitz, M.E. Hajlaoui, and R. Hajlaoui, J. Appl. Phys. 87, 4456 (2000)

S.F. Nelson, Y.Y. Lin, D.J. Gundlach, and T.N. Jackson, Appl. Phys. Lett., 72, 1854 (1998)

G. Horowitz, R. Hajlaoui, R. Bourguiga, and M.E. Hajlaoui, Synth. Metal, 101, 401 (1999)

N. Karl, J. Marktanner, R. Stehle, and W. Warta, Synth. Metal, 42, 2473 (1991)

D. Emin, Phys. Rev. Lett., 25, 1751 (1970)

T. Holstein, Ann. Phys. (N.Y.), 8, 325 (1959)

R. M. Glaser and R. S. Berry, J. Chem. Phys., 44, 3797 (1966)

G. Horowitz, Adv. Mater., 10, 3 (1998)

B. Crone, A. Dodabalapur, A. Gelperin, L. Torsi, H. E. Katz, A. J. Lovinger and Z. Bao, Applied Physics Letters, 78, 2229 (2001)

P. Peumans, V. Bulovic and S. R. Forrest, Applied Physics Letters, 76, 3855 (2000)

C. W. Tang and S. A. VanSlyke, Applied Physics Letters, 51, 913 (1987)

K. Tsukagoshi, J. Tanabe, I. Yagi, K. Shigeto, K. Yanagisawa and Y. Aoyagi, Journal of Applied Physics, 99, 064506 (2006)

Y. Chen, J. Au, P. Kazlas, A. Ritenour, H. Gates and M. McCreary, Nature, 423, 136 (2003)

Takao Someya, Yusaku Kato, Tsuyoshi Sekitani, Shingo Iba, Yoshiaki Noguchi, Yousuke Murase, Hiroshi Kawaguchi and Takayasu Sakurai, Proceedings of the National Academy of Sciences vol. 102, no. 35, 12321 (2005)

http://en.wikipedia.org/wiki/Electronic_paper referenced from Wikipedia

http://www.ntech.t.utokyo.ac.jp/Archive/Archive_download/pictures/artificial_skin3.jpg referenced from Wikipedia

B. Crone , A. Dodabalapur, Y. Y. Lin, R. W. Filas, Z. Bao, A. LaDuca, R. Sarpeshkar, H. E. Katz and W. Li, Nature vol. 403, no. 6769,521 (2000)

Zhenan Bao, Andrew J. Lovinger and Ananth Dodabalapur, Applied Physics Letters, vol. 69, no. 20, 3066 (1996)

H. E. Katz, J. Mater. Chem., vol. 7, no. 3, 369 (1997)

F. Ebisawa, T. Kurokawa, S. Nara, J. Appl. Phys. 54, 3255 (1983)[4] Z.N. Bao, Adv. Mater., 12, 227 (2000)

C.D. Dimitrakopoulos and D.J. Mascaro, IBM J. Res. Dev., 45, 11 (2001)

B. Crone, A. Dodabalapur, A. Gelperin, L. Torsi, H. E. Katz, A. J. Lovinger, and Z. Bao, Appl. Phys. Lett., 78, 2229 (2001)

L. Wang, D. Fine, T. Jung, D. Basu, H. von Seggern, and A. Dodabalapur, Appl. Phys. Lett., 85, 1772 (2004)

C.W. Tang and S. A. VanSlyke, Appl. Phys. Lett., 51, 913 (1987)

P. Peumans, V. Bulovic, and S. R. Forrest, Appl. Phys. Lett., 76, 3855 (2000)

Y. Chen, J. Au, P. Kazlas, A. Ritenour, H. Gates, and M. McCreary, Nature, 423, 136 (2003)

K. Tsukagoshi, J. Tanabe, I. Yagi, K. Shigeto, K. Yanagisawa, Y. Aoyagi, J. Appl. Phys., 99, 064506 (2006)

A. Facchetti, M. Mushrush, H.E. Katz, and T.J. Marks, Adv. Mater., 15, 33 (2003)

M. Halik, H. Klauk, U. Zschieschang, G. Schmid, W. Radlik, and W. Weber, Adv. Mater., 14, 1717 (2002)

H.E.A. Huitema, G.H. Gelinck, J.B.P.H. van der Putten, K.E. Kuijk, C.M. Hart, E. Cantatore, P.T. Herwig, A.J.J.M. van Breemen, and D.M. de Leeuw, Nature, 414, 599 (2002)

N. Koch, J. Ghijsen, A. Elschner, R.L. Johnson, J.-J. Pireaux, J. Schwartz, and A. Kahn, Appl. Phys. Lett., 82, 70 (2003)

M.D. Austin and S.Y. Chou, Appl. Phys. Lett., 81, 4431 (2002)

R. J. Chesterfield, J. C. Mckeen, C. R. Newman, P. C. Ewbank, D. A. da Silva Filho, J. – L. Bredas, L. L. Miller, K. R. Mann, and C. D. Frisbie, J. Phys. Chem. B., 108, 19281 (2004)

S. Kobayashi, T. Takenobu, S. Mori, A. Fujiwara, and Y. Iwasa , Appl. Phys. Lett., 82, 4581 (2003)

S. Kobayashi, T. Nishikawa, T. Takenobu, S. Mori, T. Shimoda, T. Mitani, H. Shimotani, N. Yoshimoto, S. Ogawa, and Y. Iwasa, Nat. Mater., 3, 317 (2004)

A. Salleo, M. L. Chabinyc, M. S. Yang, and R. A. Street, Appl. Phys. Lett., 81, 4383 (2002)

K. P. Pernstich, C. Goldmann, C. Krellner, D. Oberhoff, D. J. Gundlach, and B. Batlogg, Syn. Metals, 146, 325 (2004)

F. F. Fan, J. Yang, L. Cai, D. W. Price, Jr., S. M. Dirk, D. V. Kosynkin, Y. Yao, A. M. Rawtlett, J. M. Tour, and A. J. Bard, J. Am. Chem. Soc., 124, 5550 (2002)

Byungwook Yoo, Applications of molecular electronics to n-channel organic field-effect transistors, complementary circuits, and nanowire transistors, PhD Dissertation (2006)

I. Kymissis, C. D. Dimitrakopoulos and S. Purushothaman, IEEE Trans. Elect. Dev., 48, 1060 (2001)

D. J. Gundlach, L. L. Jia, and T.N. Jackson, IEEE Elect. Dev. Lett., 22, 571 (2001)

S.M. Sze, Physics of semiconductor devices, 2nd Ed., Wiley, New York (1981)

T.W. Lee, Y. Byun, B.W. Koo, I.N. Kang, Y.Y. Lyu, C.H. Lee, L. Pu, and S.Y. Lee, Adv. Mater., 17**,** 2180 (2005)

A. Babel and S. A. Jenekhe, J. Am. Chem. Soc., 125, 13656 (2003)

S.C. Lim, S.H. Kim, J. H. Lee, H. Y. Yu, Y. Park, D. Kim, and T. Zyung, Mater. Sci. Eng. B., 121, 211 (2005)

C. R. Newman, C. D. Frisbie, D. A. da Silva, J. L. Bredas, P. C. Ewbank, and K. R. Mann, Chem. Mater., 16, 4436 (2004)

G.H. Gelinck, H.E.A. Huitema, E. van Veenendaal, E. Cantatore, L. Schrijnemakers, J.B.P.H. van der Putten, T.C.T. Geuns, M. Beenhakkers, J.B. Giesbers, B.-H. Huisman, E.J. Meijer, E.M. Benito, F.J. Touwslager, A.W. Marsman, B.J.E. van Rens, and D.M. de Leeuw, Nature Mater., 3, 106 (2004)

J. Krumm, E. Eckert, W.H. Glauert, A. Ullmann, W. Fix, and W. Clemens, IEEE Elect. Dev. Lett., 25, 399 (2004)

M.G. Kane, J. Campi, M.S. Hammond, F.P. Cuomo, B. Greening, C.D. Sheraw, J.A. Nichols, D.J. Gundlach, J.R. Huang, C.C. Kuo, L. Jia, H. Klauk, and T.N. Jackson, IEEE Elect. Dev. Lett., 21, 534 (2000)

M. G. Pollack, A. D. Shenderov and R. Fair, Lab on a Chip, 2, 96 (2002)

Michael G. Pollack, Richard B. Fair and Alexander D. Shenderov, Applied Physics Letters, 77, 11, 1725 (2000)

O. Sandre, L. Gorre-Talini, A. Ajdari, J. Prost, and P. Silberzan, Phys. Rev. E, 60, 2964 (1999)

B. S. Gallardo, V. K. Gupta, F. D. Eagerton, L. I. Jong, V. S. Craig, R. R. Shah, and N. L. Abbott, Science, 283, 57 (1999)

T. S. Sammarco, and M. A. Burns, AIChE Journal, 45, 350 (1999)

T. B. Jones, M. Gunji, M. Washizu and M. J. Feldman, Journal of Applied Physics, 89, 2, 1441 (2001)

Kazuo Hosokawa, Teruo Fujii and Isao Endo, Analytical Chemistry, 71, 4781 (1999)

K. Handique, D.T. Burke, C. H. Mastrangelo, and M. A. Burns, Analytical Chemistry, 73, 1831 (2001)

Kunihiro Ichimura, Sang-Keun Oh, and Masaru Nakagawa, Science, 288, 1624 (2000)

M. Washizu, IEEE Trans. Ind. Applications, 34, 732 (1998)

J. Isaksson, N. D. Robinson and M. Berggren, Thin Solid Films, 515, 2003 (2006)

M. Gunji, and M. Washizu, Jrnl. of Physics D: Appl. Phys., 38, 2417 (2005)

Y.Zhao, and S. K. Cho, Lab on a Chip, 6, 137 (2006)

P. Paik, V. K. Pamula, M. G. Pollack and R. B. Fair, Lab on a Chip, 3, 28 (2003).

B. Crone, A. Dodabalapur, Y.-Y Lin, R. W. Filas, Z. Bao, A. LaDuca, R. Sarpeshkar, H. E. Katz, and W. Li, Nature, 403, 521 (2000)

http://en.wikipedia.org/wiki/Microfluidics referenced from Wikipedia

http://www.answers.com/topic/microfluidics?cat=technology

http://www.cbte.group.shef.ac.uk/research/eng2.html

http://www.eeel.nist.gov/812/MNT/activities.html

K. Handique, D.T. Burke, C. H. Mastrangelo, and M. A. Burns, Analytical Chemistry, 72, 4100 (2000)

M. A. Burns, C. H. Mastrangelo, T. S. Sammarco, F. P. Man, J. R. Webster, B. N. Johnson, B. Foerster, D. Jones, Y. Fields, A. R. Kaiser and D. T. Burke, Proc. Natl. Acad. Sci. U.S.A., 93, 5556 (1996)

J. Lee and C. J. Kim, Journal of Microelectromechanical Systems, 9, 171 (2000)

G. Beni and S. Hackwood, Applied Physics Letters, 38, 207 (1981)

E. Colgate and H. Matsumoto, Journal of Vacuum Science and Technology A, 8, 3625 (1990)

M. Vallet, B. Berge and L. Vovelle, Polymer, 37, 2465 (1996)

H. J. J. Verheijen and M. W. J. Prins, Langmuir, 15, 6616 (1999)

W. J. J. Welters and L. G. J. Fokkink, Langmuir, 14, 1535 (1998)

E. Seyrat and R. A. Hayes, Journal of Applied Physics, 90, 1383 (2001)

C. B. Gorman, H. A. Biebuyck and G. M. Whitesides, Langmuir, 11, 2242 (1995)

V. Peykov, A. Quinn and J. Ralston, Colloid Polym. Sci., 278, 789 (2000)

http://img.clubic.com/photo/012C000000296448.jpg

H. Moon, S. K. Cho, R. L. Garell and C-J. Kim, Journal of Applied Physics, vol. 92, no. 7, 4080 (2002)

S. K. Cho, H. Moon and C-J. Kim, Journal of Microelectromechanical Systems, vol. 12, no. 1, 70 (2003)

J. A. Schwartz, J. V. Vykoukal and P. R. C. Gascoyne, Lab on a Chip, 4, 11 (2004)

G. Beni and S. Hackwood, Bulletin of the American Physical Society, vol. 26, no. 3, 445 (1981)

http://csrg.ch.pw.edu.pl/tutorials/mTAS/projects.html

http://www.devicelink.com/ivdt/archive/00/11/0011i47e.jpg

http://biomechanics.ecs.umass.edu/bioMEMS.jpg

T. Krupenkin, S. Yang, and P. Mach, Applied Physics Letters 2003, vol. 82, no. 3, 316 (2003)

B. Berge and J. Peseux, Eur. Phys. J. E., 3, 159 (2003)

img.clubic.com/photo/00296453.jpg

M. G. Pollack, A. D. Shenderov and Richard B. Fair, Lab on a Chip, 2, 96 (2002)

A. Manz and H. Becker, Microsystem Technology in Chemistry and Life Sciences, Springer, Berlin, Germany (1998)

P. Gravesen, J. Branebjerg and O. S. Jensen, Journal of Micromechanics and Microengineering, 3, 168 (1993)

M. Elwenspoek, T. S. J. Lammerink, R. Mikaye and J. H. J. Fluitman, Journal of Micromechanics and Microengineering, 4, 227 (1994)

S. Shoji and M. Esahi, Journal of Micromechanics and Microengineering, 4, 157 (1994)

C. H. Mastrangelo, M. A. Burns and D. T. Burke, Proceedings of the IEEE, 86, 1769 (1998)

G. J. M. Bruin, Electrophoresis, 21, 3931 (2000)

M. Washizu, IEEE Trans. Ind. Applications, **34**, 732 (1998)

M. G. Pollack, R. B. Fair, and A. D. Shenderov, Applied Physics Letters, Vol.**77**, No.11, 1725 (2000)

Bharat Bhushan and Yong Chae Jung, Ultramicroscopy, 107, (10-11) 1033 (2007)

S. Nadkarni, and A. Dodabalapur, presented at the 47th Annual TMS Electronic Materials Conference 2005, University of California, Santa Barbara, Session Z (2005)

Jun Zeng and Tom Korsmeyer, Miniaturization for Chemistry, Biology and Bioengineering, Lab Chip, 4, 265 (2004)

H. Moon, S. K. Cho, R. L. Garrell and C-J. Kim, Journal of Applied Physics, vol. 92, no. 7, 4080 (2002)

B. Crone, A. Dodabalapur, Y. –Y. Lin, R. W. Filas, Z. Bao, A. LaDuca, R. Sarpeshkar, H. E. Katz and W. Li, Nature 403 (6769), 521 (2000)

A. Dodabalapur, Materials Today, vol. 9, no. 4, 24 (2006)

M. Kitamura and Y. Arakawa, Applied Physics Letters, 91, 053505 (2007)

B. Yoo, T. Jung, D. Basu, A. Dodabalapur, B. A. Jones, A. Facchetti, M. R. Wasielewski and T. J. Marks, Applied Physics Letters,88, 082104 (2006)

B. Yoo, D. Basu, T. Jung, D. Fine, B. A. Jones, A. Facchetti, M. R. Wasielewski, T. J. Marks, K. Dimmler and A. Dodabalapur, presented at the 64th Annual Device Research Conference (2006)

G. A. de Wijs, C. C. Mattheus, R. A. de Groot and T. T. M. Palstra, Synthetic Metals, 139, 109 (2003)

M. Pope and C.E. Swenberg, Electronic Processes in Organic Crystals and Polymers, 2nd edition, Oxford University Press, New York, 1999, 337-340

Hagen Klauk, David J. Gundlach, Jonathan A. Nichols and Thomas N. Jackson,
IEEE Transactions on Electron Devices, vol. 46, no. 6, 1258 (1999)

Y.-Y. Lin, D. J. Gundlach, S. F. Nelson and T. N. Jackson, IEEE Transactions on Electron Devices, vol. 44, no. 8, 1325(1997)

B.A. Jones, M. J. Ahrens, M.-H. Yoon, A. Facchetti, T.J. Marks, and M.R. Wasielewski, Angew. Chem. Int. Ed., 43, 6363 (2004)

A. Salleo, M. L. Chabinyc, M. S. Yang, and R. A. Street, Applied Physics Letters, vol. 81, no. 23, 4383 (2002)

B. K. Crone, A. Dodabalapur, R. Sarpeshkar, R.W. Filas, Y.Y. Lin, Z. Bao, J. H. O'Neill, W. Li, and H.E. Katz, J. Appl. Phys., 89, 5125 (2001)

Byungwook Yoo, Ashwin Madgavkar, Brooks A. Jones, Suvid Nadkarni, Antonio Facchetti, Klaus Dimmler, Michael R. Wasielewski, Tobin J. Marks and Ananth Dodabalapur, IEEE Electron Device Letters, 27, 9, 737 (2006)

Suvid Nadkarni and Ananth Dodabalapur, Journal of Materials Science: Materials in Electronics, 18, 9, 931 (2007)

Suvid Nadkarni, Byungwook Yoo, Debarshi Basu and Ananth Dodabalapur, Applied Physics Letters, 89, 184105 (2006)

S. K. Cho, H. Moon and C.-J. Kim, Journal of Microelectromechanical Systems, 12, 1, 70 (2003)

J. A. Schwartz, J. V. Vykoukal and P. R. C. Gascoyne, Lab Chip, 2, 96 (2002)

Jun Zeng and Tom Korsmeyer, Lab on a Chip, 4, 265 (2004)

M. Vallet, B. Berge and L. Vovelle, Polymer, 37, 12, 2465 (1996)

M. Washizu, IEEE Trans. Ind. Applications, 34, 732 (1998)

M. G. Pollack, A. D. Shenderov and R. Fair, Lab on a Chip, 2, 96 (2002)

VITA

Suvid Vikas Nadkarni was born in Pune, India on March 23, 1981, the son of Manjiri Vikas Nadkarni and Vikas Madhusudan Nadkarni. He completed elementary, middle and high school from Loyola High School and Junior College, Pune, India in 1998. He received his bachelor's degree as a Bachelor of Engineering in Electronics and Telecommunications Engineering from the Pune Institute of Computer Technology, affiliated to the University of Pune, in May 2002. He joined the University of Texas at Austin in August 2002 for graduate studies in Electrical Engineering. He received his M.S. in Electrical Engineering in May 2004 and continued his study for a Ph.D. in Electrical Engineering at the Microelectronics Research Center as a Graduate Research Assistant under the supervision of Dr. Ananth Dodabalapur. In the summer of 2005, he worked as an intern at SEMATECH, Austin.

Permanent Address: A-18 Garden Estate, Off D. P. Road, Aundh, Pune 411 007, India.

This dissertation was typed by Suvid Vikas Nadkarni.